INVESTIGATING SOLID-STATE SUPERCAPACITORS CONSTRUCTED WITH PVA/CNT NANOCOMPOSITE ELECTROLYTES

A Thesis by

Temmuz Coskun

Bachelor of Science, Wichita State University, 2012

Submitted to the Department of Mechanical Engineering
and the faculty of the Graduate School of
Wichita State University
in partial fulfillment of
the requirements for the degree of
Master of Science

May 2014

INVESTIGATING SOLID-STATE SUPERCAPACITORS CONSTRUCTED WITH PVA/CNT NANOCOMPOSITE ELECTROLYTES

The following faculty members have examined the final copy of this thesis for form and content, and recommend that it be accepted in partial fulfillment of the requirement for the degree of Master of Science with a major in Mechanical Engineering.

_____
Ramazan Asmatulu, Committee Chair

_____
Hamid Lankarani, Committee Member

_____
Mehmet Bayram Yildirim, Committee Member

DEDICATION

To my mother, father, and soon-to-be wife

ACKNOWLEDGEMENTS

I would like to thank my advisor, Dr. Ramazan Asmatulu for his everlasting support and mentoring throughout the duration of this work. Also, I would like to extend my sincere gratitude to the members of my committee, Dr. Hamid Lankarani and Dr. Mehmet Bayram Yildirim, for their valuable comments and suggestions on this work. I would like to recognize that this project could not be possible without Dr. Asmatulu and the Department of Mechanical Engineering, Wichita State University proving facilities and resources. I would also like to thank Dr. Anil Mahapatro for providing me with testing equipment, and Department of Chemistry, Wichita State University, for providing me with materials essential for my work. Also, I would like to thank Tom McGuire from the Department of Engineering, Wichita State University, for broadening my knowledge about capacitive behavior and electrical measurement methods. My sincere appreciation goes out to my fellow researchers Aybala Usta, Amir Jabbarnia, Vamsidhar Patolla, and Muhammet Ceylan for their helpful cooperation and encouragement. Finally, I would like to thank my family, without them I would not be here; and my fiancée Emily, for helping me keep my sanity throughout this project.

ABSTRACT

The search for alternative energy generation methods requires development for new energy storage methods as well. The ability to use nanotechnology to achieve high surface area, which is correlated to increased energy storage, brought advancements in supercapacitor applications. Supercapacitors have the potential to charge and discharge quickly and hold as much energy as batteries and other chemical storage devices. By having a completely solid-state supercapacitor, problems with leakage and decay could be avoided. Supercapacitors were assembled from electrodes made by reducing graphene oxide in a computer disc drive and adhering two electrodes with composite electrolytes having various concentrations of PVA/CNT. Tests were performed on the completed supercapacitors, as well as the individual components. The analysis of the different concentrations of carbon nanotubes in PVA electrolytes showed the lowest resistivity for 0.5wt% CNT (294 Ωcm) and the highest specific capacitance for 1.0wt% CNT (123.5 F/g). This specific capacitance is a 27% improvement on an electrolyte without CNT. The electrolyte with pure PVA has similar capacitance to other solid-state supercapacitors in the literature. Electrolytes with higher percentages of CNT (0.5%) show higher resistivity because of the decreased carbon solubility or agglomerations. The final product supercapacitors, thin, flexible, and environmentally friendly, can be used in wide temperature ranges, and have a theoretically long lifespan. They can charge more quickly than batteries, and hold more energy than capacitors. This study shows promising enhancements in solid-state supercapacitors, making them an even more plausible replacement for batteries in the near future. The improvements made on the specific capacitance with the different electrolytes could lead to greater efficiency and lower cost in many unique applications requiring absence of liquid components.

TABLE OF CONTENTS

TABLE OF CONTENTS (cont'd)

Chapter Page

TABLE OF CONTENTS (cont'd)

LIST OF FIGURES

LIST OF FIGURES (cont'd)

Figure Page

LIST OF TABLES

Table Page

CHAPTER 1

INTRODUCTION

1.1. Motivation

The earth's resources are dwindling, and the burning of the fossil fuels is a main source of carbon dioxide emissions. Not only does the scarcity of the fossil fuels drive prices higher, but greenhouse gases and carbon dioxide emissions also cause climate change. There are major developments in renewable energy methods. Whether it is hybrid cars or solar panels, an electrical energy storage device should be developed to keep up with the newly invented electricity generation methods.

Batteries and capacitors are two of the most widely used energy storage devices. Batteries possess high energy densities, but low power densities. They can provide energy for a long period of time, but cannot deliver high power in a shorter period of time. Batteries also have long charging times. Capacitors can deliver pulses of energy and can be charged and discharged easily. However, the amount of energy delivered is so small, the applications that can utilize capacitors are limited.

A recent device called a supercapacitor could possibly achieve best of both worlds. By having high power density and high energy density, supercapacitors are able to deliver high power electricity over a longer period of time compared to conventional capacitors. Although they cannot yet store as much energy as batteries, the hope is that this will change in the future, given the infancy of the technology. Also, supercapacitors already exhibit higher life cycles and wider operating temperature ranges compared to batteries.

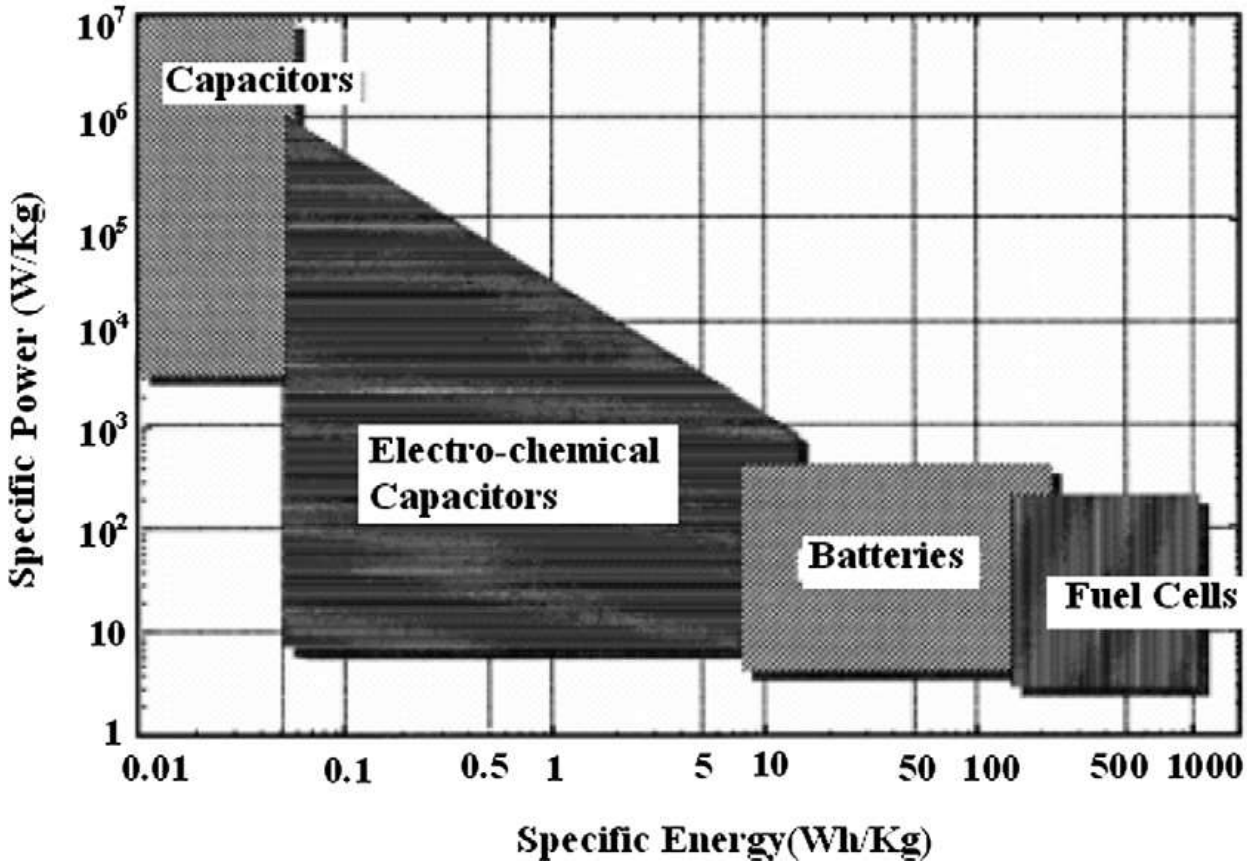

Figure 1.1 – Ragone plot of energy storage systems [1].

Figure 1.1 is a Ragone plot of electrochemical storage systems. Ragone plots are used to demonstrate the performance of energy storage systems on a log chart of power vs. energy [2]. As illustrated in the figure above, supercapacitors fill a gap where other energy storage devices do not fall. Instead of replacing a current storage method, supercapacitors fill a new niche with their unique properties.

Supercapacitors operate on the same principle as conventional electrostatic capacitors; therefore, it is worth describing how a conventional capacitor works. Capacitors are formed by two conductive materials separated by a dielectric material. When an electric potential is applied, the conductors accumulate charge. The reason supercapacitors have conductive properties is

because of the use of nanotechnology. Being able to design materials on a nanoscale allows for properties that are crucial to the improvement of capacitance values. Higher surface area and thinner materials both contribute to their performance.

Although the first supercapacitor was constructed decades ago, the demand from the emerging alternative energy market is the main reason supercapacitors are recently becoming more studied. As mentioned above, nanomaterials made supercapacitors more feasible compared to other storage devices.

1.2. General Background

The first patent of supercapacitors dates back to 1957 by General Electric [3]. The first commercially available product that utilized the supercapacitor name was by Nippon Electric Company (NEC) in the 1970s. Another company, Pinnacle Research Institute (PRI) called their product an ultracapacitor. Both of these names are still used, but they refer to the same device, a capacitor that stores energy in the interface between an electrolyte and an electrode [1]. Finally, after years, the research and the prevalence of supercapacitors increased significantly in the 1990s since new applications required quick surges of energy with great reliability [4]. Supercapacitors still only occupy less than 1% of the market for electrical energy storage. In 2007, the supercapacitor market generated a revenue of $99.6 million, and with an annual compound revenue growth of 10.9%, the revenue generated will be up to $205.9 million in 2014 [5]. Supercapacitors have had important roles in energy storage fields as a back-up power supply for some time now. The application variety of this technology is growing by the day. Supercapacitors were used in the emergency doors of the Airbus A380 to provide the surge of power needed to utilize them [6]. A report by the US Department of Energy puts supercapacitors in the same importance category as batteries for future energy storage methods [6].

1.3. Research Objectives

The goal of this thesis was to study properties of solid-state supercapacitors because of the simplistic construction, unique scope of applications, and significant room for improvement. Synthesizing and analyzing different compositions and concentration of electrolytes was a main focus in the supercapacitor construction. Improving the properties of the electrolyte would lead to a significant improvement on the properties of the supercapacitor.

There are several names for supercapacitors, such as ultracapacitor, supercap, dynacap etc. but they all appeared from branding and mean the same thing. For consistency throughout this thesis the term supercapacitor was used. Also, the supercapacitor samples in the experiments are referred to by the weight percentage of CNT they contain. In the first part of the thesis, background information about supercapacitors was provided. In the second part of the thesis, the experimental section, the trials and procedures used to achieve better electrical properties in solid-state graphene supercapacitors were explained.

CHAPTER 2

LITERATURE REVIEW

2.1. Principles of Supercapacitors

As in every energy storage device, power and energy values determine the characteristics of supercapacitors. Power and energy in supercapacitors can be mathematically explained. The maximum energy storage of a supercapacitor E can be found using the following equation [7]:

$$E = \frac{1}{2} C U^2 \quad (1)$$

In Equation 1, C is the specific capacitance, and U is the maximum cell voltage. The maximum power of a supercapacitor P can be found with the following equation [7]:

$$P = \frac{U^2}{4R_S} \quad (2)$$

U is the maximum cell voltage in this equation as well, and R_s is the equivalent series resistance. Therefore, the energy and the power of the supercapacitor are greatly affected by the maximum voltage that can be applied on it. The maximum power is also affected by the equivalent series resistance, which is related to the electrode conductivity, electrolyte resistance, contact resistance between the electrodes and the current collector, and the ionic resistance of the separator.

2.2. Advantages of Supercapacitors Compared to Batteries

Supercapacitors have several strengths compared to batteries. First of all, they exhibit higher power density. According to Figure 1, supercapacitors can exhibit power densities up to 10kW/kg, whereas batteries only reach 150W/kg. Supercapacitors possess higher power densities

than batteries because they can be charged within seconds while it takes batteries a few hours to charge [8].

Supercapacitors have longer life expectancies because, unlike batteries, there is no faradaic reaction that takes place, with the exclusion of faradaic supercapacitors. Though they still exhibit longer life cycles than batteries, they are not the focus of this study. Supercapacitors do not need to be maintained and can withstand up to 1,000,000 charge and discharge cycles and have an estimated life expectancy of 30 years compared to batteries, withstanding only 10,000 cycles with a life expectancy of 5 to 10 years [8, 9]. Longer shelf life is another advantage of supercapacitors. Batteries that are not used for extended periods of time will corrode and degrade. On the other hand, supercapacitors will retain their original condition for several years [8].

Supercapacitors have reversible charge and discharge cycles with little heat loss, getting around 95% efficiency [8, 9]. Supercapacitors can also operate in a wide range of temperatures, ranging from -40^{o}C to 70^{o}C. This allows for a wide variety of locations where supercapacitors can be utilized [8]. Supercapacitors are also environmentally friendlier than batteries. They do not contain hazardous materials like lead and are generally easy to dispose of [8].

2.3. Supercapacitor Models

Our understanding of what is occurring in supercapacitors with electrical charges and discharges, as with many things in science, took many years and different models to uncover. There are three main models that were detrimental in the current understanding of how a supercapacitor works. Figure 2.1 visualizes the current model and particle potentials, which encompasses the three models talked about in this section.

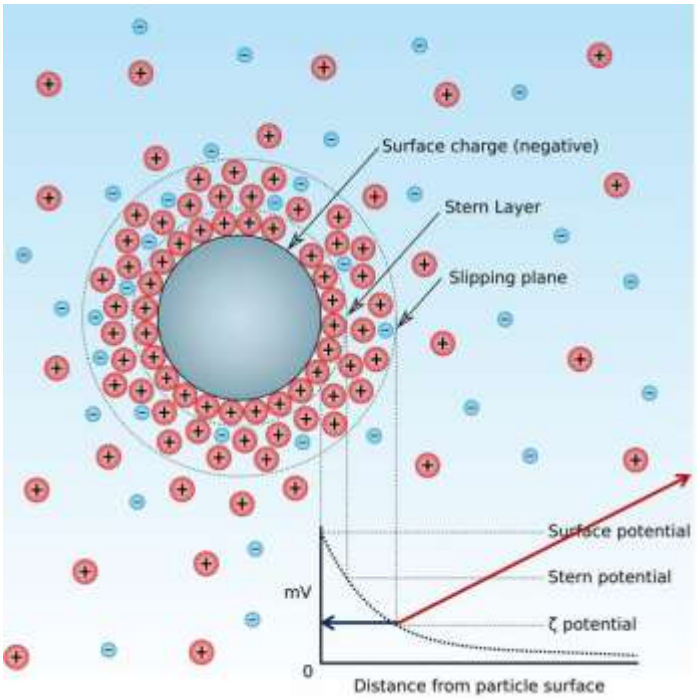

Figure 2.1: The surface charges and potential of a particle immersed in a liquid [10].

2.3.1. Helmholtz

Helmholtz was the first person to model the reaction between a conductor and an electrolyte in relation to capacitance properties. He also was the first person to use the term "double layer" [11]. The model considers the electrode as a solid plate, therefore, causing the interface to have parallel plate capacitor behavior [4]. The electrode would acquire positive charge on its surface, and a negative charge would form on the surface of the electrolyte, countering the positive charge. Figure 2.2 shows the parallel plate behavior and the charge formation associated with it.

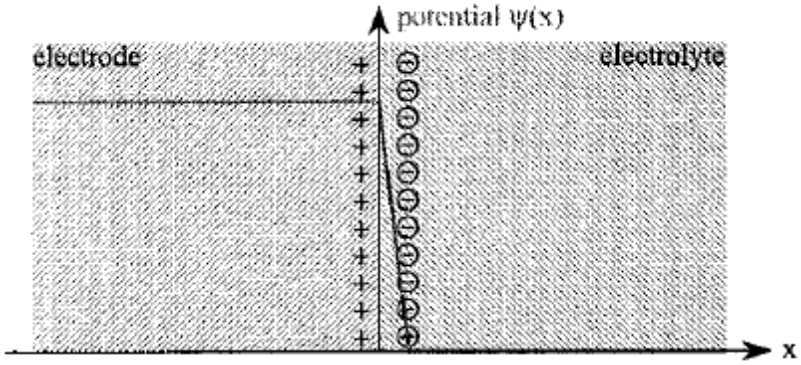

Figure 2.2 - Helmholtz double layer model [11].

This would happen the same way on the other electrode, but with opposite charges, hence why the term double layer came about. This equation calculates the capacitance in the Helmholtz model [11]:

$$C = \frac{\varepsilon}{d} \tag{3}$$

Where C is the capacitance determined solely by the dielectric constant ε of the electrolyte, and d is the double layer thickness. What this model fails to take into account is the voltage dependence of the capacitance, thus not only considering capacitance a constant, but also giving higher theoretical results [11].

2.3.2. Gouy-Chapman

Gouy acknowledged that capacitance is not constant, and that it is dependent on the voltage applied. In 1910, he described random thermal motion, which would create a space distribution of the ions in the electrolyte. Today, this phenomenon is called the diffuse layer, which is demonstrated in Figure 2.3 [11].

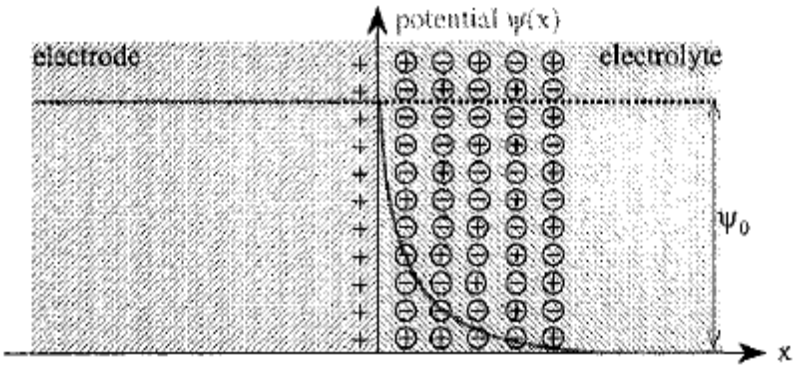

Figure 2.3 - Gouy-Chapman double layer model [11].

In 1913, Chapman formulated the diffuse layer mathematically by combining the Poission equation and the Boltzman distribution function. He came up with the following equation [11]:

$$C = z\sqrt{\frac{2qn_0\varepsilon}{u_T}}ch(\frac{z\psi_0}{2u_T}) \quad (4)$$

$$u_T = \frac{kT}{q} \quad (5)$$

In this equation, the capacitance C is dependent on the surface potential ψ_0, the valence of electrolytic ions z, the anion and cation concentration at thermodynamic equilibrium n_0, the Boltzmann constant k, and the temperature T. This model considers ions to be point charges, which means, in theory, that they could be infinitely close to the interface, causing an increased theoretical capacitance.

2.3.3. Stern

Stern's model combines the Helmholtz and the Gouy-Chapman models [4]. It separates the charge into the Helmholtz compact layer and the Gouy-Chapman diffused layer. Figure 2.4 shows the combination of the compact layer and the diffused layer on the electrode-electrolyte interface.

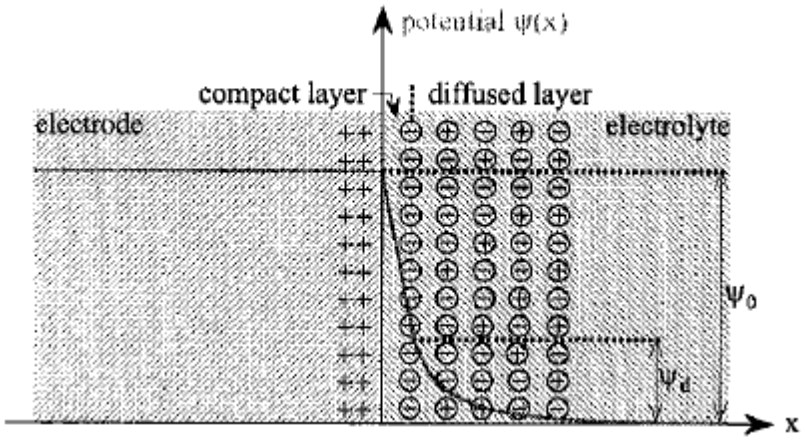

Figure 2.4 - Stern double layer model [11].

The Stern model uses an equation that combines the two previous models [11]:

$$\frac{1}{C} = \frac{1}{C_c} + \frac{1}{C_d} \quad (6)$$

Capacitance is determined by two main components, where C_c is the Helmholtz compact layer, and C_d is the Gouy-Chapman diffuse layer with the exception that the surface potential ψ_d is used instead of ψ_0 [11].

2.4. Types of Supercapacitors

Supercapacitors can be divided into two groups depending on the means by which the charge is stored. The type of electrode materials used in the supercapacitor determines the type of supercapacitor.

2.4.1. Electric Double Layer Supercapacitor

Electric double layer supercapacitors (EDLS) use materials that are not electrochemically active; therefore, the charging and discharging is an entirely physical reaction [5]. Surface dissociation and ion adsorption allow the charge to be stored on the electrodes [6]. This happens only on the surface, rather than the whole electrode. When an external electrical charge is

applied, the electrons in the negative electrode move to the positive electrode. At the same time positive ions move to the negative electrode from the positive electrode. This exchange takes place through the electrolyte. Since there are no chemical reactions taking place, the process happens fast and does not create degradation on the cell, increasing the life of the supercapacitor way beyond the lifespan any other chemical storage device could achieve.

2.4.2. Faradaic Supercapacitors

Faradaic supercapacitors (FS), also called pseudocapacitors, utilize fast, reversible redox reactions to store energy, a process that resembles a lithium-ion battery [12]. Unlike EDLS, the charge and discharge process happens throughout the electrode, instead of only the surface. This allows for higher capacitance values, and as a result, comparatively higher energy density. This comes at the price of lower power density than EDLS because the faradaic redox reactions occur more slowly than electrostatic processes [13].

2.5. Electrodes

2.5.1. Background

Electrodes are often considered the most important component of supercapacitors, since the electrical properties heavily depend on the electrode materials and construction. Whether a supercapacitor is electrochemical double layer or faradaic is also determined by the electrode material used.

Surface area of the electrode has a huge influence on capacitance values of supercapacitors. However, the capacitance does not increase linearly with the surface area because not all of the surface area is accessible during the charge and discharge process. Hence,

the term “electrochemically accessible surface area” is used to define the area that is in direct relation to capacitance [5].

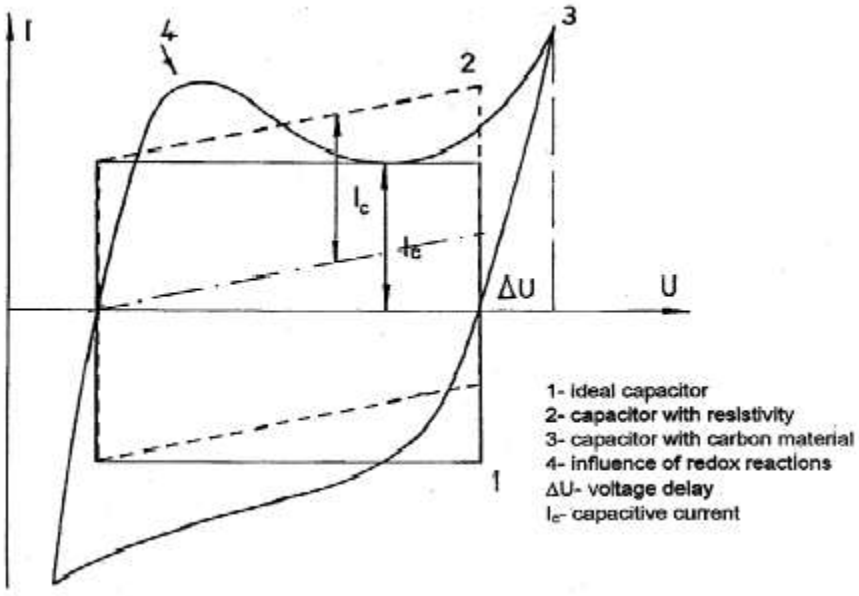

Figure 2.5 – Cyclic Voltammetry diagram of different capacitors [14].

In order to inspect and measure capacitance behavior of electrodes, cyclic voltammetry is a reliable and often used method. Figure 2.5 compares the curves different electrode materials create on a cyclic voltammetry graph. An ideal capacitor will plot a perfect rectangular shape, but under real world conditions, the shape will become a parallelogram because of resistances. In the case of electrodes that undergo a faradaic reaction during charge and discharge, such as transition metal oxides and conductive polymers, the curve will gain deviate further from the rectangle and causing peaks because of the redox reactions that occur.

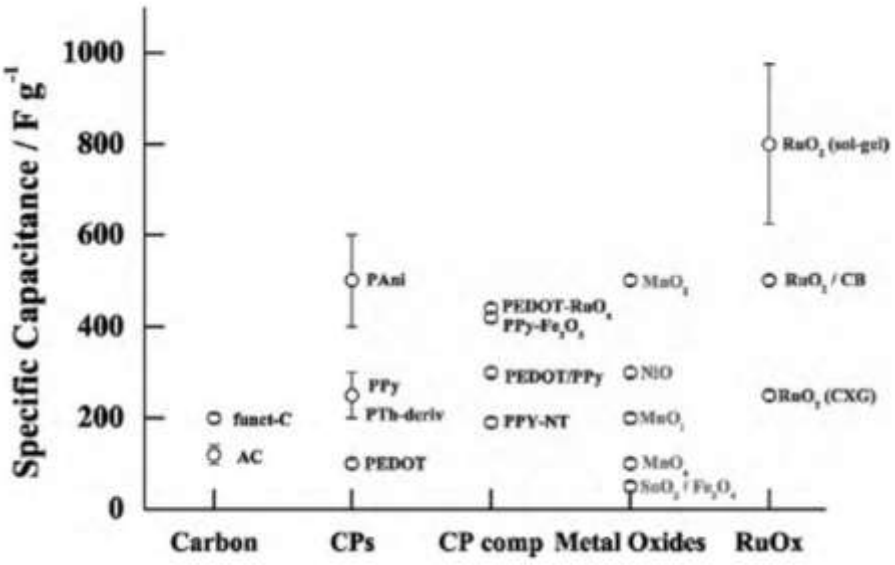

Figure 2.6 - Comparison of specific capacitance values of different electrode types [15].

Figure 2.6 compares the capacitance values of different electrode materials. Faradaic materials clearly achieve higher capacitance values, but a number of other things must be taken into consideration while choosing an electrode material. For example, faradaic materials suffer from shorter life cycles, and ruthenium oxide, which shows the highest capacitance value in the chart, is too expensive to ever be in a commercial supercapacitor.

2.5.2. Transition Metal Oxides

Transition metal oxides (TMOs) are popular electrode materials for supercapacitors because they can achieve high capacitance values because of the way they collect charge. Metal oxides do not only collect electrostatic charge on the electrode, but they also undergo fast redox reactions on the electrode material in order to achieve extra charge. A good electrode will have an electrically conductive oxide, as well as a metal that can exist in two or more oxidation states possessing the ability to co-occur through a continuous range without undergoing irreversible

phase changes [16]. Also, the protons need to be able to enter and exit oxide lattice during the redox reaction [5]. Most notable metal oxides used as electrode materials are: RuO_2, MnO_2, PbO_2, NiO_x, V_2O_5 and Fe_3O [4].

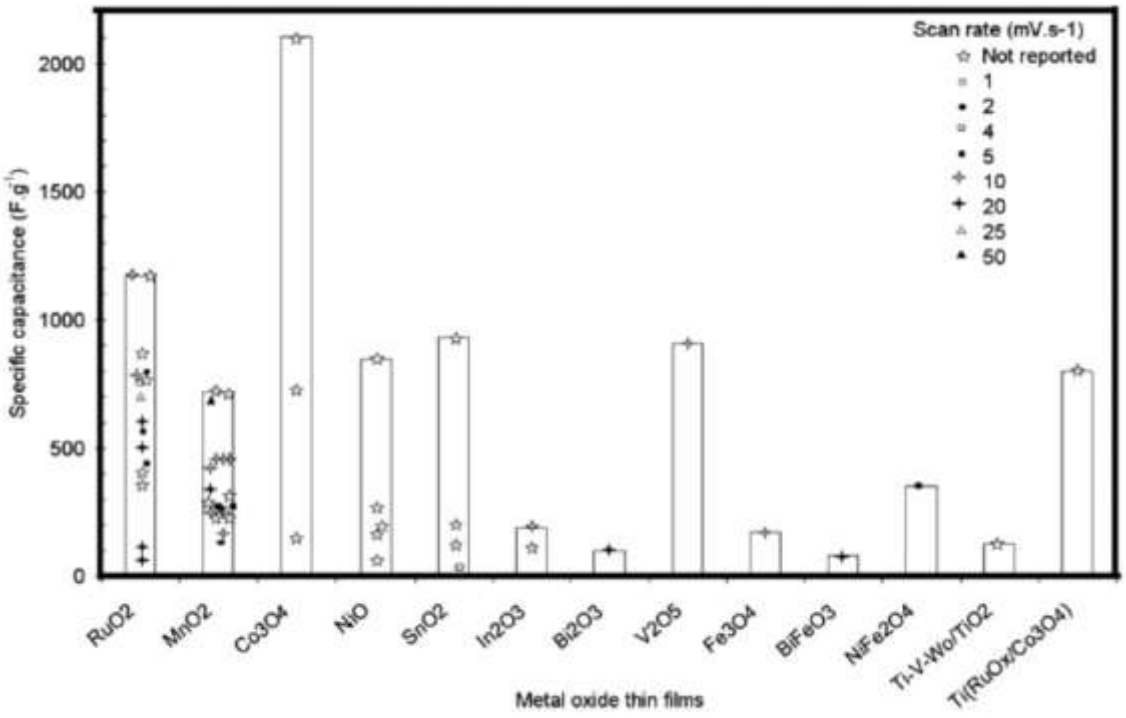

Figure 2.7 – Specific Capacitance Values of TMOs investigated with various scan rates [16].

As seen in Figure 2.7 above, TMOs can achieve extremely high specific capacitance values. However, the high cost of the metals used limit viable commercial applications, especially in the cases of Ruthenium Oxide and Vanadium Oxide, where the capacitance values are amongst the highest [17].

2.5.3. Conductive Polymers

Conductive polymers (CPs) are also viable materials for supercapacitor electrodes. They have lower cost and impact on the environment than TMOs [18]. They have high conductivity, a

high voltage window, and a high storage capacity [18, 19]. CPs achieve capacitance via highly reversible redox reactions. Oxidation and reduction reactions cause the ions to enter and exit the backbone of the polymers. This occurs throughout the entire electrode instead of just the surface, hence high specific capacitance values can be achieved [20]. However, since the ions enter and exit the conductive polymer electrodes with a redox reaction, it causes them to swell and shrink, eventually leading to cracks and damage. This severely affects the capacitance, therefore, limiting the cycle life of capacitors made by conductive polymers [21].

CPs need to be either positively or negatively "doped" with ions in order to reach the conductivity levels suitable for an electrode material. This is done by an oxidation or reduction process. Polymers become positively charged after the oxidation process, and are then called "p-doped." When reduction happens, they become negatively charged hence the name "n-doped" [5]. There are three types of supercapacitors that can be constructed entirely with conductive polymer electrodes, classified as Type I, Type II, and Type III. Type I is a symmetric supercapacitor that uses identical p-dopable polymer electrodes, Type II is an asymmetric supercapacitor that utilizes different p-dopable polymers, and finally Type III is a symmetric supercapacitor that uses the same polymer but with a p-doped positive and an n-doped negative electrode [15, 22-24]. The most common conductive polymer electrodes are constructed with polypyrrole, polyaniline, and polythiophene variants [25].

2.5.4. Carbons

Since the prehistoric era, humans have always used carbon materials to generate or store energy. Whether it was burning charcoal to generate heat using graphite in construction of lithium ion batteries, carbon has been a necessary part of human life [26]. In the field of supercapacitors, the significance of carbon materials can be observed or as well. Carbon is the

most popular electrode material used in supercapacitors and assumed to have a bright commercial future. The advantages include, but are not limited to, abundance, low cost, high specific surface area, non-toxicity, good conductivity, high chemical stability, and wide operating temperatures [7, 27]. Carbon compounds are used in electrochemical double layer supercapacitors, storing the charge in the electrode surface-electrolyte interface. Consequently, surface area and pore size distribution are extremely important, as well as electrical conductivity.

Pore size of carbon materials is directly related to the capacitance of the supercapacitors, since it is one of the key components that make surface area electrochemically active. Studies done by Largeot et al. [28] show that the capacitance value is highest when the pore size is close to the size of the ions in the electrolyte. As the pore size gets larger or smaller, the capacitance drops considerably.

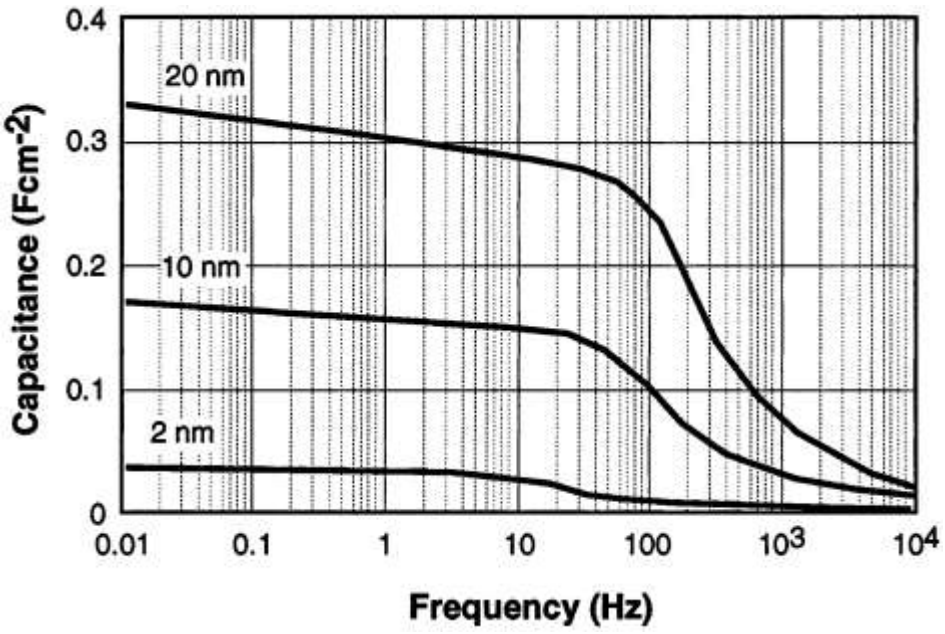

Figure 2.8 – Capacitance vs Frequency plot for carbon electrodes with differing pore sizes [29].

Figure 2.8 illustrates the relation of pore size to capacitance. With pore sizes too small compared to electrolyte ions, there is virtually no capacitance, especially in higher frequencies. However, the increase of the pore size diameter, while keeping the electrolyte pore number constant leads to an increase in capacitance, as well as an increase in the higher operational frequency window [29]. The pore size of the carbon electrodes are controllable with the types of precursor materials used as well as the type of activation/functionalization method. The temperature, time, and chemical agents used are all factors affecting the porosity of carbons [7]. A wide variety of carbons can be used as electrodes including, but not limited to, activated carbons, templated carbons, graphene, carbon nanotubes, carbon black, carbon aerogels, and carbon nanoparticle composites [1, 5-8].

2.5.5. Graphene Electrodes for Supercapacitors

With a theoretical specific surface area of 2675 m^2/g [30], and controllable pore size, graphene is an ideal electrode material. However, the theoretical value has yet to be attained experimentally. During the synthesis of graphene and related devices, the individual sheets of graphene start aggregating and severely reducing the surface area [31]. There are a variety of different methods that researchers utilized in order to increase surface area and capacitance values. The preferred method is the reduction of graphene oxide to graphene. Graphene oxide is a popular choice since its precursor is graphite, which is readily available and inexpensive. In 1957, Hummers et al. [32] treated graphite with sulfuric acid, sodium nitrate, and potassium permanganate in order to achieve graphitic oxide, which is the same thing as graphene oxide. This process is named the Hummers Method, and it was later modified by adding another oxidization stage and improving its outcomes [33]. After graphene oxide is obtained, there are a number of different ways to go about the reduction to graphene.

Chemical Reduction of Graphene Oxide

Graphene oxide flakes can be suspended in water, and the resulting suspension can be reduced with chemical methods. Stankovich et al. [34] reduced graphene oxide into graphene by reacting it with hydrazine hydrate. This simple and inexpensive method resulted in thin graphene sheets with some agglomeration and a surface area of 466 m^2/g, which is promising, but nowhere near the theoretical value of graphene. Chen et al. [35] used a weaker reductant, hydrobromic acid, which resulted in an impressive specific capacitance of 348 F/g in an aqueous electrolyte. This is attributed to the weaker reducing agent leaving more stable oxygen groups intact, increasing wettability; therefore, the surface area the electrolyte could reach was increased substantially.

Thermal Reduction of Graphene Oxide

Graphene oxide can also be reduced by heat. Under normal conditions, temperatures of 550^oC and higher will exfoliate graphene oxide sheets and cause reduction [36, 37]. Vivekchand et al. [38] created graphene electrodes by thermally reducing graphene oxide at 1050^oC. Acquired graphene sheets had a specific surface area of 925m^2/g and capacitance up to 117 F/g in an aqueous medium. Nevertheless, this process uses a lot of energy, and it is not efficient compared to the alternatives.

Graphene Nanoparticle Composites

Since the biggest reason for surface area loss is attributed to stacking of the graphene sheets, attaching nano-particles in between the layers as spacers could diminish agglomeration greatly [31, 39-41]. Because of its great electrical properties, platinum is used as a spacer in

between graphene sheets. This is done by adding chloroplatinic acid with a surfactant and reductants into a graphene oxide suspension in water. The chemical reaction taking place reduces both graphene oxide and platinum by attaching the particles onto the sheets [39-41]. Figure 2.9 compares the graphene sheets with and without the nanoparticle spacers. It can be seen that the spacers prevent the graphene sheets from sticking to each other.

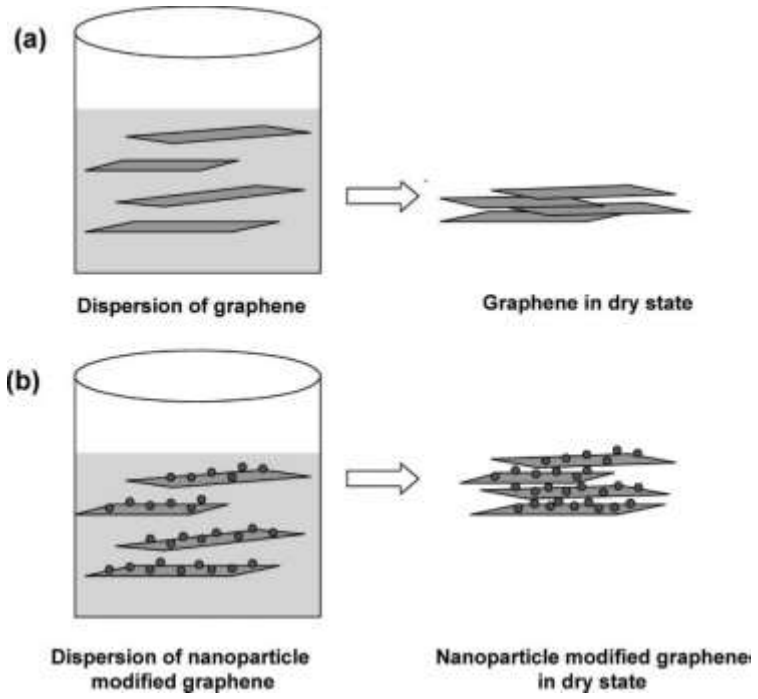

Figure 2.9 – Dispersed and dried graphene with and without nanoparticle spacers [31].

Laser Irradiation of Graphene Oxide

An interesting method that was invented recently is the reduction of graphene oxide by infrared lasers. El-Kady et al. [42] used an inexpensive LightScribe CD burner in order to reduce graphene oxide. Graphene oxide suspension is dried on a PET sheet which is attached to a disc and put through the burning process. The resulting film has a conductivity of 1738 S/m and a specific surface area of 1520 m^2/g.

2.6. Electrolytes

Electrolytes occupy the space in between the electrodes and allow ions to move through them. It is a notably important component in constructing a supercapacitor because the highest operational voltage depends on the breakdown voltage of the electrolyte, which is squarely proportional to both the energy and the power densities of the supercapacitor [1]. Electrolyte also impacts the equivalent series resistance (ESR), which is a determinant of the power density.

A suitable electrolyte should have a wide voltage window, high electrochemical stability, high ionic concentration, low solvated ionic radius, low resistivity, low viscosity, low volatility, low toxicity, low cost, and availability at high purity [5]. There are three types of commercially available electrolytes: Aqueous electrolytes, organic electrolytes, and ionic liquids. The fourth type of electrolyte, the solid electrolyte, is not common in the industry.

2.6.1. Aqueous electrolytes

Aqueous electrolytes are composed of aqueous solutions of acids. The common aqueous electrolytes are 1 mol L^{-1} H_2SO_4 and 6 mol L^{-1} KOH [11]. Aqueous electrolytes allow supercapacitors reach higher conductivity values compared to their non-aqueous counterparts. However, a significant drawback is the low voltage window; the thermodynamic window of water shows decomposition at only 1.23 V [23].

2.6.2. Organic Electrolytes

Organic electrolytes can exhibit drastically higher operating voltages than their aqueous counterparts. Solvents in organic electrolytes can dissolve larger quantities of salt, which leads to a major advantage. Unfortunately, they fall short in terms of environmental friendliness. Commonly used organic solvents are acetonitrile and propylene carbonate. Supercapacitors containing organic electrolytes can theoretically operate at 3V [43].

2.6.3. Ionic Liquids

Ionic liquids are salts that are in liquid form under operating conditions. Unlike the aqueous and organic electrolytes, ionic liquids do not require a solvent. They have desirable characteristics like high ionic conductivity, low vapor pressure, a wide electrochemical window, and high thermal stability [15]. They are also non-flammable, making them safer for use. The paramount quality of ionic liquids is the electrochemical stability, allowing operating voltages of 4V and beyond [44].

2.6.4. Solid Electrolyte

Electrolytes play an important role in supercapacitors. However, the fact that they are the only liquid component of supercapacitors is an unfortunate drawback [45]. Since supercapacitors contain liquids, they need to be handled and packaged properly with strong encapsulation [45-47]. This limits the variety of applications for supercapacitors. Additionally, using liquids always causes a risk of leakage, one that increases as the life cycle comes to an end [45].

If a solid electrolyte is used, an all solid-state supercapacitor that is flexible and durable can be synthesized. Solid electrolytes also open a new window of applications, like wearable electronics. Solid-state supercapacitors are much safer and more suitable for portable applications than their liquid counterparts. An electrolyte in solid form can usually be achieved by using gelled or solid polymers [45]. The polymer gel is then mixed with a conducting acid, resulting in a polymer matrix filled with a conductor. To compare it with a liquid electrolyte, it can be said that the polymer works as the separator where the conductor works as an ionic liquid.

2.7. Separator

The separator is a thin film that is sandwiched between the electrodes in order to prevent contact between them. Choice of the separator depends on the electrolyte used; ceramic or glass

fiber separators are used for aqueous electrolytes, and polymer or paper separators are used for organic electrolytes [1]. Separators must prevent electrical contact between electrodes but also allow the ions to transfer during charge and discharge. Ideal separators for application with supercapacitors will have high electrical resistance, good ionic permeability, and low thickness [48]. Common materials used to construct separators are rubber, plastic, aquagel, nafion, polypropylene, and polyolefin films [49].

2.8. Applications

Although supercapacitors are fairly new to the market and are currently in development stages, supercapacitors are already utilized or are in the process of being implemented in a number of applications.

Supercapacitors are especially useful in applications that demand energy for short periods of time. Batteries and conventional capacitors fail to provide a favorable amount of power in a time frame that is limited to seconds or minutes. This results in the need to combining a lot of batteries or capacitors in packs to achieve the required power, causing a waste in materials and space. Applications that use short bursts of energy tend to utilize these bursts frequently. The large number of cycles would cause batteries to wear out and require frequent replacements, whereas supercapacitors could withstand many cycles without substitution.

2.8.1. Backup Memory

Supercapacitors are readily utilized in appliances that have digital memory storage. In the case of an interruption of the power supply, the supercapacitor acts as a backup power supply for the short period of time until power is restored [1]. An alarm clock functioning through a power outage is a good example.

2.8.2. Electric / Hybrid Vehicles

An increase in research and development in alternative energy systems for motor vehicles has been seen because better fuel efficiency will not only be beneficial for the consumer, but also the environment. According to the Environmental Protection Agency, motor vehicles cause one half of smog-forming volatile organic compounds, more than half of the NOx emissions, about half of the toxic air pollutant emissions, and 75 percent of CO emissions in the United States [50].

Fuel cells are considered to be a suitable candidate for powering motor vehicles in the future. As can be seen in Figure 1.1, fuel cells clearly possess the highest energy density amongst the energy storage devices. These properties would allow enough energy for long-distance travel. On the other hand, fuel cells have low power density and lack the capabilities required for energy recuperation [51]. Coupling with another energy storage device would be needed in order to provide power to start the car, accelerate rapidly, and recoup energy from braking [51-53].

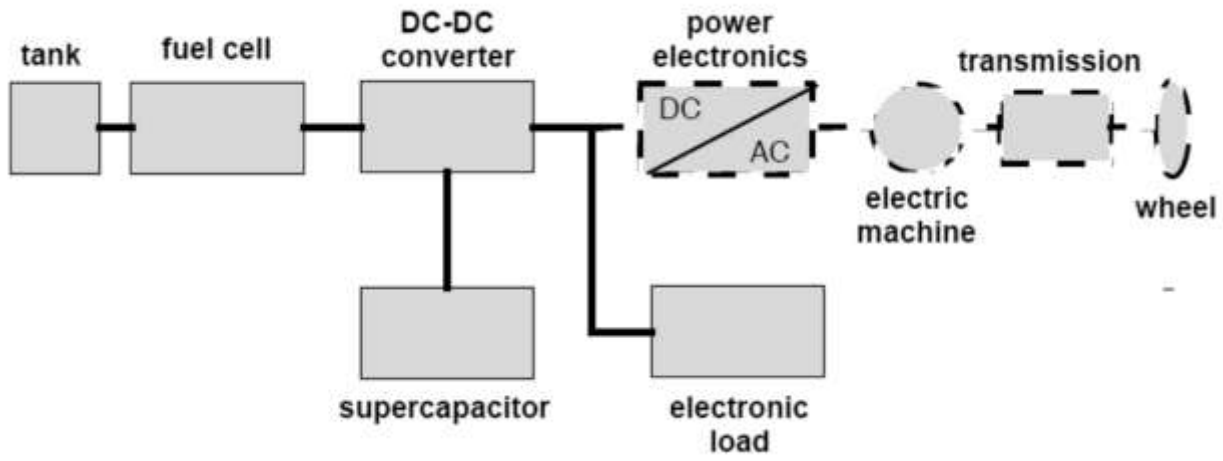

Figure 2.10 – Fuel cell-supercapacitor power system for vehicles [52].

Figure 2.10 shows the electric power train studied by Kötz et al. [51, 52] which combines a 6.5kW fuel cell stack and a10kW supercapacitor stack. The system provides a smooth flow of power throughout the operation of the motor vehicle. When there is rapid acceleration, the supercapacitor releases the energy, and when braking occurs, the energy generated is directed to the supercapacitor.

2.8.3. Power Quality

Electromechanical oscillation is a problem that occurs in power plants, specifically in electric generation and distribution terminals that can cause partial or even complete power interruptions [54]. These oscillations are controlled by damping. STATCOM (Status Synchronous Compensators) is a system that is designed to control damping. STATCOM will take power from the system or give power to the system depending on the need. To control disturbances effectively, a storage device with high power density is needed; to compensate for longer lasting oscillations, a storage device with high energy density is needed. Supercapacitors are a great candidates for STATCOM because they have these necessary properites. Although they still have comparatively limited storage, the voltage disturbances generally do not exceed 10 cycles and the speed of charging and discharging still makes supercapacitors better candidates than batteries [55].

2.8.4. Battery Monitoring

Batteries are used every day in our laptops, cell phones, and other portable electronics. If a portable device is used long enough, noticeable decline in the battery performance will occur, and eventually a replacement will be needed. This occurs because batteries draw currents that can have short, high bursts. Combining batteries with supercapacitors will allow the

supercapacitor to shield the battery by taking in the burst loads [56]. This protective measure will extend the life of the battery.

2.8.5. Portable Power Supplies

Although it is not feasible today, ideally, supercapacitors will be able to power portable electronics by themselves. Replacing batteries with supercapacitors would lower charging times significantly and increase the operational temperature range. However, supercapacitors only have 15-20% energy density of batteries which is required for long term energy supply [57]. Also, the current capital cost of a supercapacitor is 5-20 $/kJ, where the capital cost of batteries is 0.3-2 $/kJ [57]. The cost will have to significantly decrease for the industry to implement supercapacitors in commercial products

2.8.6. Electrochemical Actuators

To be able to fit within the constraints of the current potential applications, it is beneficial for electrical actuation systems to be compact and lightweight; the smaller and lighter the power source, the better [58]. To be able to cut down on size without sacrificing performance, power and energy densities need to be as high as possible. The process in actuation systems usually involves high pulse peak power, but a moderate power for average use [59]. Creating a hybrid energy storage system with batteries and supercapacitors would not only allow us to meet the energy and power densities, but it also save on size and weight, up to approximately 60% in one case [57].

2.8.7. Integrating in Renewable Energy

Although there has been considerable advancement in the renewable energy field, the majority of the world's energy demand is still satisfied by fossil fuels. Multiple reasons are preventing renewable energy methods like solar panels from completely taking over, like high cost and low efficiency. While the energy generation efficiency is increasing every day in such devices, the storage efficiency is failing to keep up with this increase. Incorporating supercapacitors, as opposed to batteries, into a photovoltaic energy system will increase efficiency; a battery may lose up to 30% of the energy during charging, but a supercapacitor will lose 10% or less [57]. The wider operating temperatures will also allow the use of photovoltaic panels in more locations with colder or warmer climates [1].

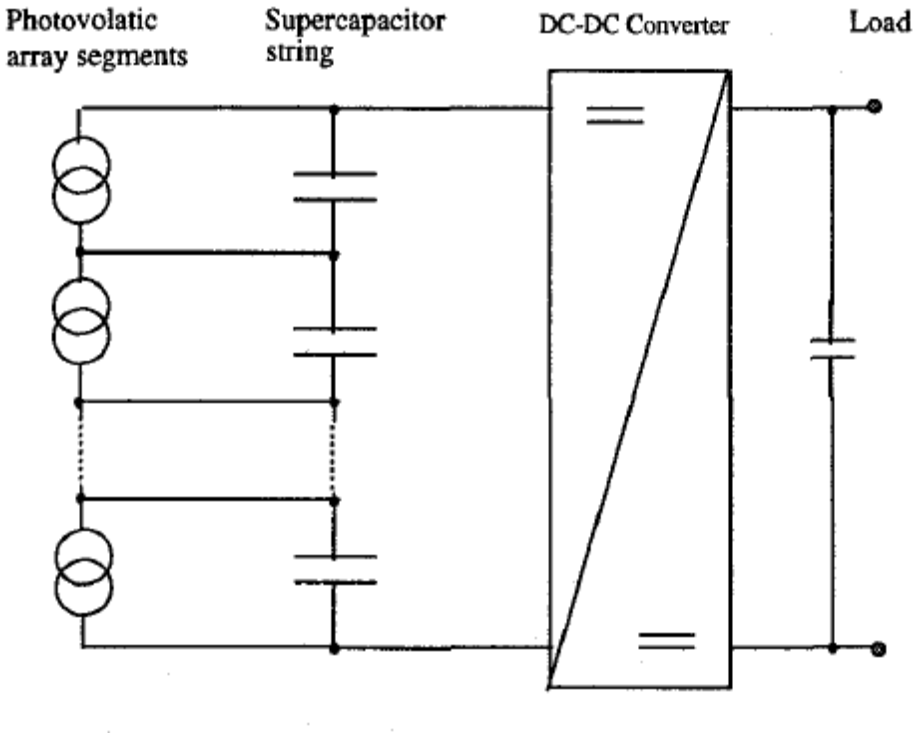

Figure 2.11 – Photovoltaic/Supercapacitor power system [59].

In Figure 2.11, a system that powers telecommunications network units is shown [60]. In this system, a supercapacitor is connected to each photovoltaic cell, where both the supercapacitor and the photovoltaic cell share the same voltage rating. The string of the supercapacitors delivers a high voltage load to the dc-dc converter which then delivers the load in the required voltage. In order to provide energy to a larger application, like an entire building, a hybrid system consisting of photovoltaic, supercapacitor, and fuel cells can be used [61]. The fuel cells will provide the energy density needed for longer periods of energy usage, where the supercapacitor will be able to boost the power when necessary.

2.9. Nanomaterials

2.9.1. Graphene

The 2010 Nobel Prize in Physics was awarded to Geim and Novoselov for their work with graphene [62]. Graphene is a two-dimensional sp^2 hybridized carbon material that is packed into a honeycomb lattice [63, 64]. Essentially, grapheme is a 2D form of graphite. In fact, graphene was prepared for the first time by peeling layers out of a graphite sheet until a single layer of atoms was left [65]. In contrast, if graphene sheets are manually stacked on top of each other, graphite will be formed. Graphene demonstrates impressive properties, like great mechanical strength, high electrical and thermal conductivity, and large surface area [30]. These properties make graphene a strong candidate for many applications, supercapacitors being one of them.

2.9.2. Carbon Nanotubes

Another member of the carbons with the sp^2 hybridization that has drawn much attention is the carbon nanotube. It was discovered by Ijima in 1991while performing laser ablation [66].

Since then, more methods to produce carbon nanotubes have been established, such as chemical vapor deposition, the arc method, hyrdrocarbon catalytic decomposition, electrolysis, and pyrolysis [67, 68]. Carbon nanotubes possess outstanding physical properties with a Young's modulus of 1200 GP, and a tensile strength of 150 GPa [69]. In addition to their favorable physical properties, CNT also demonstrates exceptional electrical properties, with a theoretical carrier mobility of 10,000 cm^2/Vs and an electrical current density of 4×10^9 A/cm^2 [70].

2.9.3. Nanotechnology Safety and Concerns

Nanomaterials improve the quality and the efficiency of many applications they are utilized in. Even though it is beneficial to use nanomaterials to construct electrochemical storage devices, there are risks associated to human health and environment that needs to be considered. As nanomaterials become more and more common, an effort to study the risks is required. Also, both the risks and benefits need to be known and accepted by society [71].

CHAPTER 3

EXPERIMENTAL

3.1. Materials

3.1.1. Electrode

Figure 3.1 shows the materials that were used to construct the electrode. Single-Layer Graphene Oxide (GO) (99% Purity, 0.7-1.2 nm thickness) was purchased from GOOGRAPHENE in Alexandria, Virginia. Polyethylene terephthalate (PET) film was manufactured by MG Chemicals (416-T PET Transparency Film Sheet). The film thickness is 0.1 mm and it is thermally rated up to 392^{o}F, which does not create a barrier for high temperature applications. Bare conductive paint is a water based paint that becomes conductive as it dries.

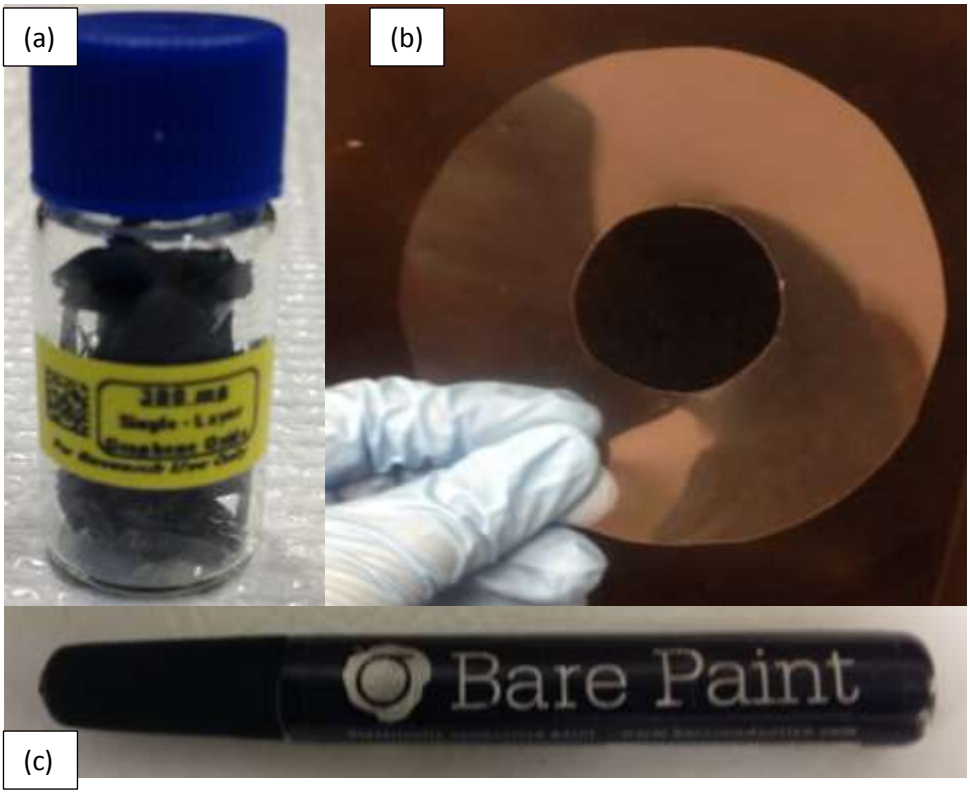

Figure 3.1 – a) Graphene Oxide by GOOGRAPHENE b) PET sheet by MG Chemicals cut in the shape of a LightScribe disc c) Bare conductive paint

3.1.2. Electrolyte

Polyvinyl alcohol (PVA) powder was purchased from Aldrich Chemistry (99+% hydrolyzed). Catalytic multi-wall carbon nanotubes (140nm diameter) were purchased from MER Corporation. Phosphoric acid (85% H_3PO_4) by Fisher Scientific was provided by the Wichita State University Department of Chemistry. Figure 3.2 shows the materials used.

Figure 3.2 – (a) PVA by Aldrich (b) MWCNT by MER (c) Phosphoric Acid by Fisher Scientific.

3.2. Methods

3.2.1. Graphene Oxide Reduction

A PET sheet was cut into the shape of the area that can be labeled on a LightScribe disc. This shape is similar to a regular disc, but the only difference is the diameter of the hole in the center, which is slightly larger in order to fit the encoding strip for the driver to read.

Figure 3.3 – a) Harrick Plasma Cleaner PDC-32G and b) Fisher Scientific FS60D Sonicator used in experiments.

To help the GO adhere more completely, the PET sheet was processed with the Harrick Plasma Cleaner (Figure 3.3.a) for 3 minutes. Plasma cleaning the PET sheet removes contaminants, creates a hydrophilic surface, and enhances adhesion [72]. 50 mg of GO flakes were added into a 150ml beaker. 13.5 ml of de-ionized (DI) water was added into the beaker to achieve a 100mg GO/27 ml water ratio [42]. The beaker was put into a Fisher Scientific sonicator (Figure 3.3.b) for 2 hours to disperse the GO in water homogeneously. The top of the

beaker was covered with parafilm to prevent excess water from dripping into the flask, like the water that condenses under the lid of the sonicator after heat build-up. The water used in the sonicator was also replaced every 30 minutes to prevent overheating. The sonicated GO/water dispersion was dropcasted onto the PET film on level ground and dried overnight at room temperature.

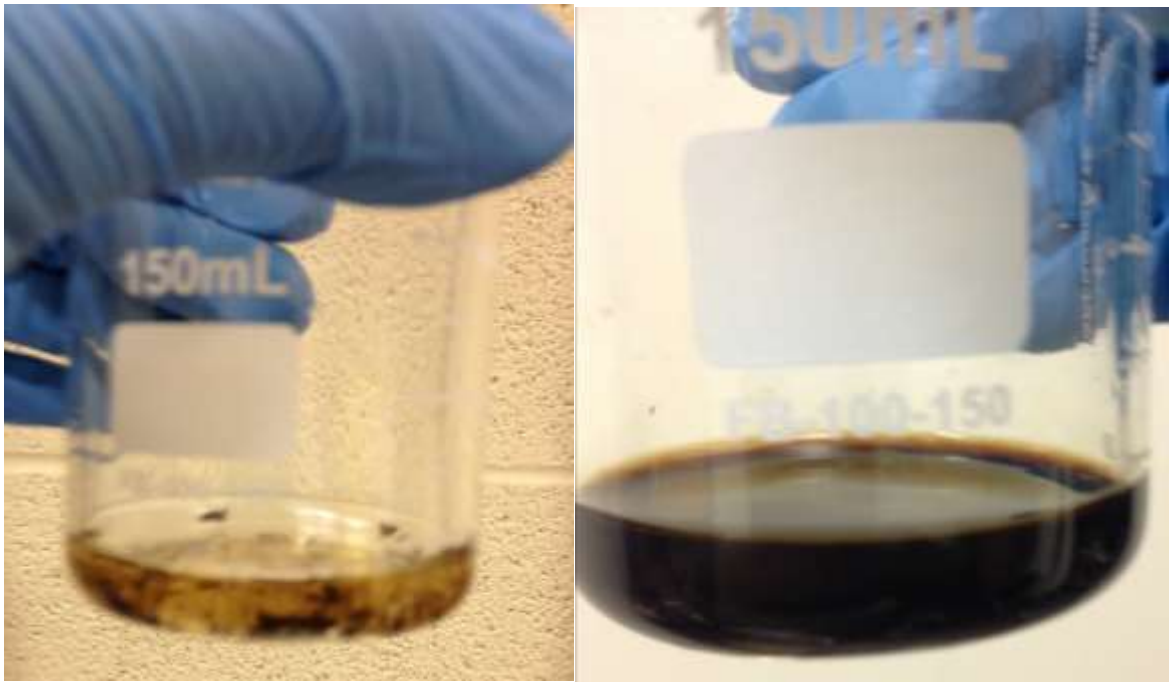

Figure 3.4 – Graphene oxide dispersion in water before and after sonication.

The graphene oxide was reduced using a LightScribe system. LightScribe is an optical disc labeling technology created by Hewlett-Packard that utilizes discs coated with a special dye that changes color under infrared laser light [73]. When graphene oxide is subjected to the same infrared laser, reduction occurs by exfoliation. A LightScribe disc was coated with spray adhesive and the dried GO/PET film was applied to the disc. The disc was then inserted into the drive and underwent the burning process.

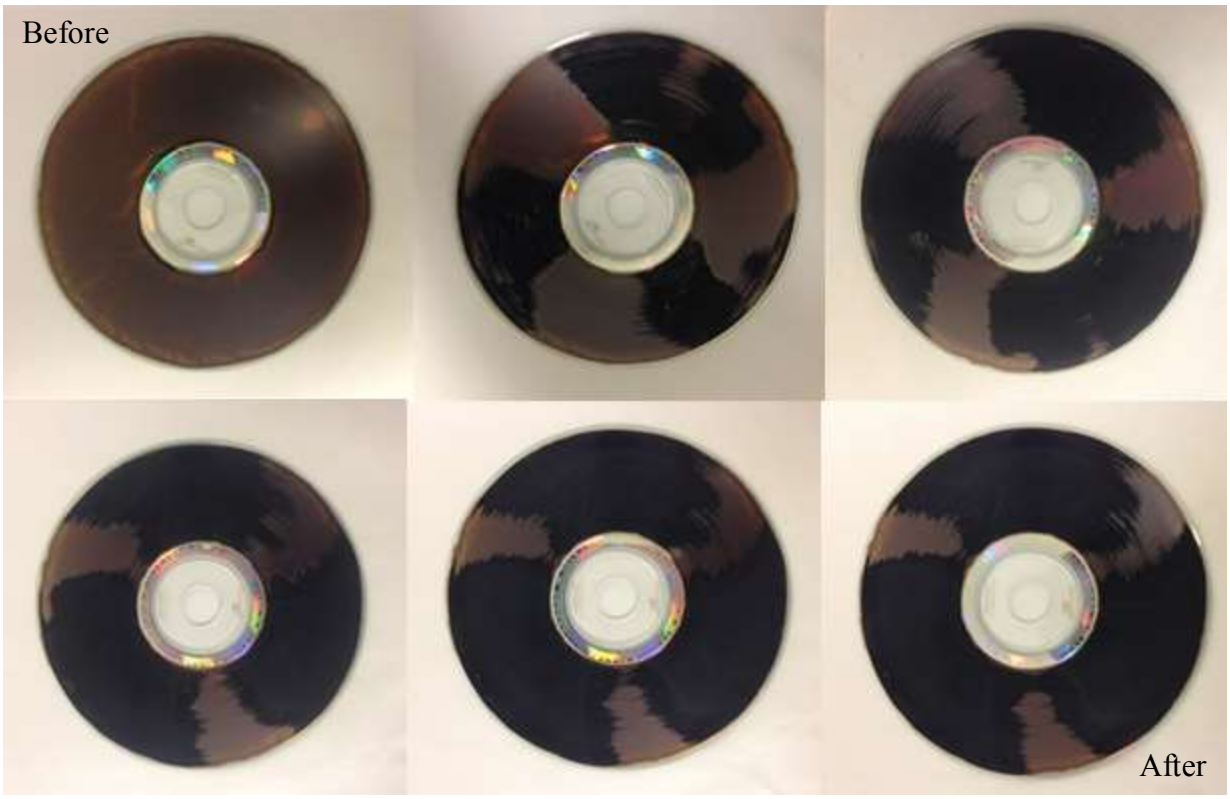

Figure 3.5 – The burning steps of graphene oxide nanofilm.

Figure 3.5 displays the outcome of each step of the burning process. The CD goes through the LightScribe labeling process between 4 to 6 times, until the graphene oxide is fully reduced or until the reduced area ceases to increase in size. Each cycle in the LightScribe labeling process lasts 22 minutes, with the software programmed to burn the entire surface area of the disc. Afterwards, the PET/graphene film was carefully removed from the disc with a box cutter or an x-acto knife.

3.2.2. Constructing the Polymer Electrolyte

Deionized water was heated to 90^{o}C. Under constant stirring, PVA powder with a 1:10 weight ratio of powder to water was added extremely slowly. It was important to carefully execute this step because as the powder comes into contact with water, it will swell and become

sticky, causing agglomeration if added too quickly. Therefore, very few PVA particles could be added at once in order for dissolution to occur. The solution was mixed with mechanical agitation under constant heat until all the PVA was mixed thoroughly. By visually inspection, the homogeneity of the solution can be determined. The color of the solution will change from white to clear, and there will be no visible PVA particles floating in the beaker. Next, an equal weight of phosphoric acid in respect to the PVA powder was added. The solution was stirred for an additional hour to ensure a homogenous mixture.

3.2.3. Creating PVA/CNT Electrolytes

In order to clean the particles, carbon nanotubes (CNT) were mixed with acetone and sonicated for 1 hour. Afterwards, the mixture was heated to 60^{o}C and kept at that temperature until all of the acetone evaporated and only left carbon nanotubes in powder form [74]. In the meantime, the PVA mixture was being stirred on the hot plate at 60^{o}C.

In the next step, a pre-determined amount of the CNT powder was added to the mixture. The mixture was stirred for 1 hour. Following the stirring, the solution was sonicated for a predetermined amount of time. After sonication, the solution was stirred for 1 more hour on the hot plate at 60^{o}C. During sonication, air bubbles will form in the solution, and the stirring afterwards ensures air bubbles escape, as well as giving extra time for dissolution. This step was repeated for every electrolyte with different amounts of CNT in solution and different sonication times listed in Table 3.1

Table 3.1 – Parameters for creating CNT/PVA composites

CNT weight % in relation to PVA	Total weight of CNT (g)	Amount of CNT added since the step before (g)	Sonication time (minutes)
0.1%	0.003	0.003	120
0.5%	0.015	0.012	150
1%	0.03	0.015	180
2%	0.06	0.03	240

When each electrolyte mixture was prepared, a small amount of it was dropcasted onto a plasma cleaned PET sheet in order to obtain thin films for inspection and measurements. The films can be seen in Figure 3.6 with no CNT on the left, 2% CNT on the right, and increasing in weight percentages in between.

Figure 3.6 – Photographs showing the electrolyte thin films.

3.2.4. Assembly of Supercapacitors

Two identical electrodes were built with Laser Scribed Graphene (LSG) for every supercapacitor. PET film was used as a backing for the electrodes, doubling as the outside shell of the supercapacitor. The electrodes are created by cutting the film into a 2 x 2 cm square shape with a tab extending on one side of the square which was used to clamp alligator clips. For a

single capacitor, two identical electrodes are required, as illustrated in Figure 3.7. When the graphene side of the electrodes is facing upward, the tab for the clamps should be on the same side of each square.

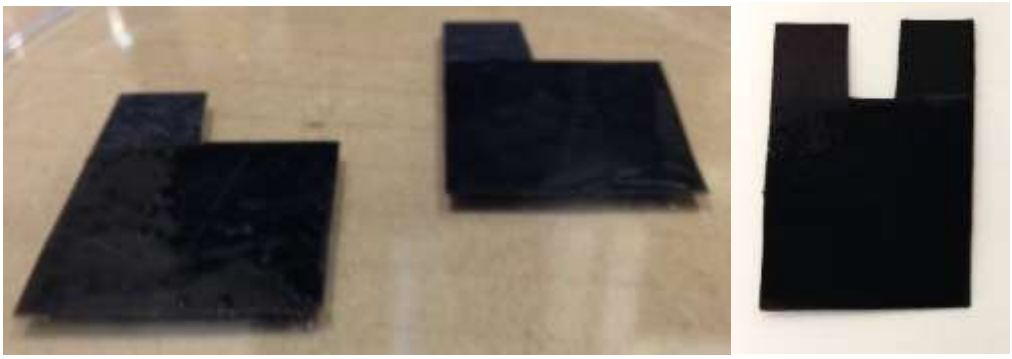

Figure 3.7 – Supercapacitor electrodes while they were drying, and the finished product.

For every supercapacitor, the respective electrolyte mixture was carefully applied on the electrode surface with a brush, carefully avoiding the tab. The electrodes were then left in 25^{o}C temperature for 2 hours. This accomplishes two important things: First of all, it allows the electrolyte to wet the electrode surface, achieving higher surface areas that are accessed by the electrolyte. Secondly, drying allows any water that might be left in the mixture to evaporate. This is crucial because any water left will decrease the maximum voltage that can be applied and increase the resistance of the capacitor. Finally, Bare Conductive Paint was applied to the tabs of the electrodes in order to prevent the alligator clips from damaging the graphene. The cross section of the finished supercapacitors is demonstrated in Figure 3.8. After the electrolyte was allowed to dry for 2 hours, one electrode was flipped over and pressed on the PVA side of another electrode, leaving the PET on the outside of the capacitor, and the electrolyte sandwiched between. This figure is not scaled.

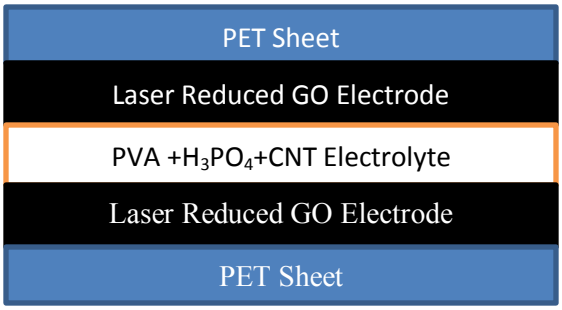

Figure 3.8 – The cross sectional view of supercapacitor setup.

3.3. Characterization

3.3.1. Scanning Electron Microscopy

Scanning Electron Microscopy (SEM) inspections were performed with a Carl Zeiss Sigma VP Field Emission Scanning Electron Microscope (Figure 3.9). GO/PET film was inspected with the microscope before and after the reduction process. The thin films coated exclusively in electrolyte were inspected as well.

Figure 3.9 – Scanning Electron Microscope used in the current study.

3.3.2. Cyclic Voltammetry

Cyclic voltammetry (CV) is a widely used electro-analytical method in electrochemistry. Cyclic voltammograms are obtained by introducing a potential excitation signal and measuring the response current at the working electrode [75]. Typically, in cyclic voltammograms, the y-axis displays the current, while the x-axis displays potential. Since the potential changes over time, x-axis can also be assumed as the time axis.

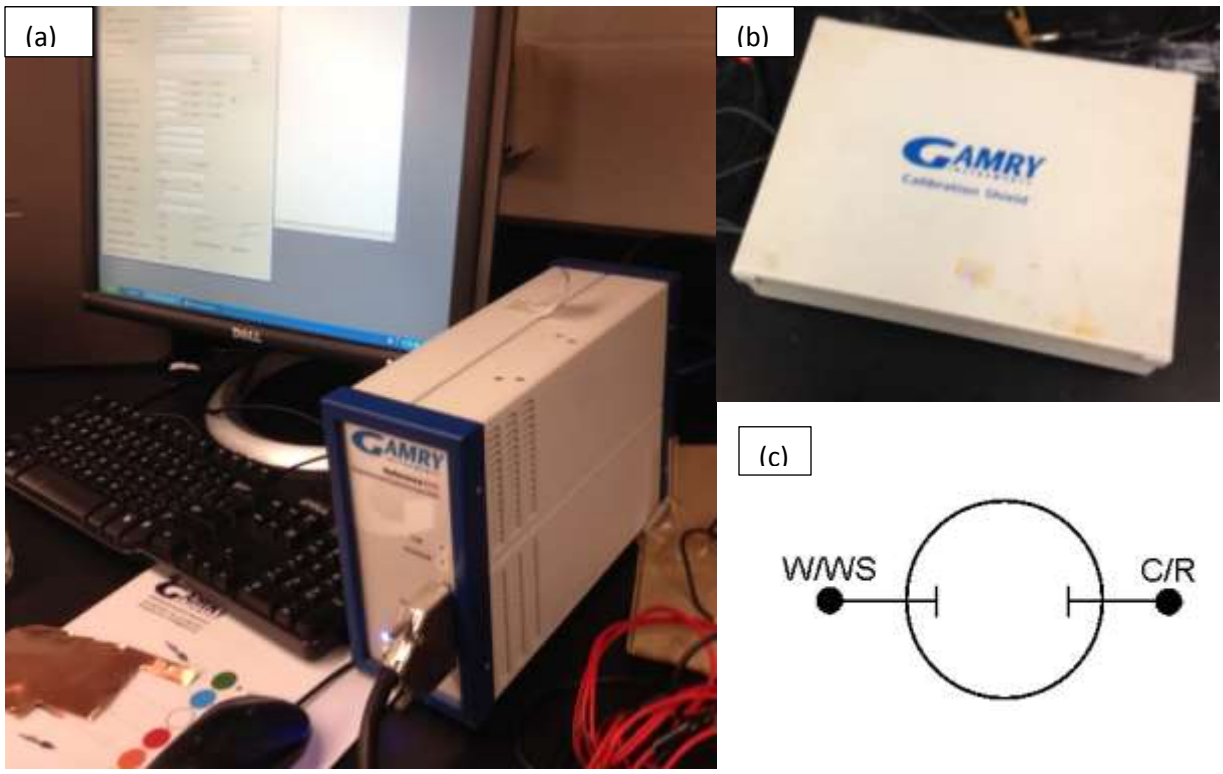

Figure 3.10 – (a) Gamry Reference 600 (b) Faraday cage (c) Two electrode setup for Gamry Reference 600 [76].

Cyclic Voltammetry was carried out with Gamry Reference 600 Potentiostat/Galvanostat /ZRA (Figure 3.10.a). Two-electrode setup demonstrated by Gamry [76, 77] was chosen for the measurements since it was the only viable option with an all solid system and a scan rate of 100mV/s was used. One electrode was designated as the working electrode by connecting the

working and the working sense probes to it. The remaining electrode was designated as the reference by connecting the reference and the counter probes to it (Figure 3.10.c). Since all the supercapacitors measured were symmetrical, designating which electrode was working and which one was the reference was not necessary. Additionally, the system was setup in a Faraday cage in order to block any outside interference (Figure 3.10.b)

3.3.3. Resistivity Measurements

Electrolyte resistance measurements were done with GWINSTEK GDM-8034 Digital Multimeter pictured in Figure 3.11. Each sample was measured three times to improve accuracy. Resistivity values were obtained later with calculations demonstrated in Appendix D.

Figure 3.11 - GWINSTEK GDM-8034 Digital Multimeter used in the resistance measurements.

3.3.4. Charge/Discharge Behavior

The charging and discharging behaviors of the supercapacitors were observed with the Tektronix TDS 2002C Oscilloscope. Voltage versus time plots were observed in order to see the effects of charging, discharging, and resistance.

Figure 3.12 - Tektronix TDS 2002C Oscilloscope used in observing charge and discharge.

CHAPTER 4

RESULTS AND DISCUSSION

4.1. SEM Analysis

Although the difference between the graphene oxide sheet before and after the LightScribe process can be visibly seen, the reduction can be further confirmed with Scanning Electron Microscopy (SEM). In Figure 4.1.a and 4.1.b, the GO resting on the PET film can be observed in differing magnification levels. It is worth noting that the GO is transparent enough for the PET to be observed in the pictures as well. In Figure 4.1.c and 4.1.d, the reduced GO can be observed at the same magnification levels. Before reduction, there was a relatively flat surface with limited surface area. However, after reduction the surface became exfoliated and the surface area greatly increased. During the inspection of the GO sheet with SEM, an interesting reaction occurred. When the magnification level increased further than the level in Figure 4.1.b, a reduction mechanism was initiated. The reduction of the GO sheet could be observed in real time; however, the magnification level was lowered in order to protect the device from damage. The full sized SEM images of the electrode samples can be found in Appendix A.

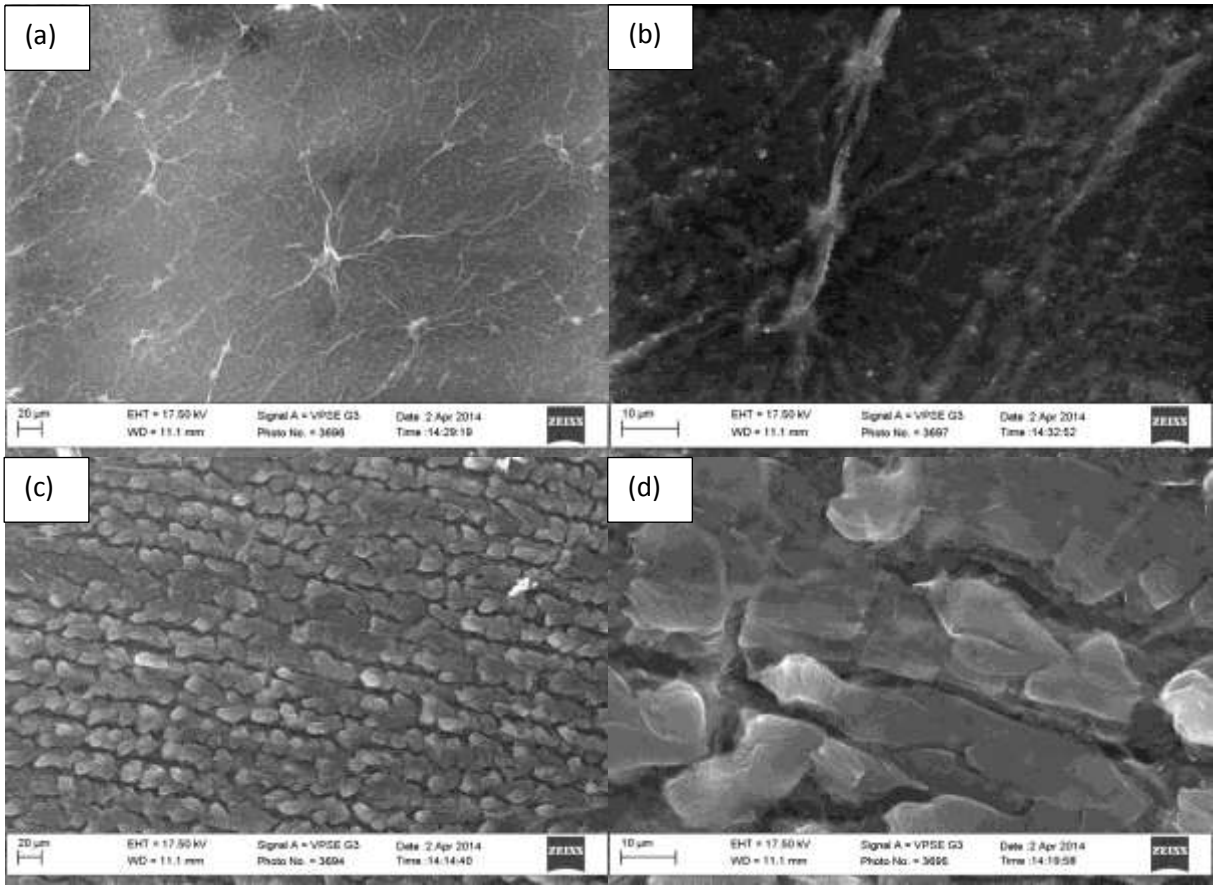

Figure 4.1 – SEM images of (a) Graphene oxide (b) Graphene oxide in higher magnification (c) Laser reduced GO and (d) Laser reduced GO in higher magnification.

In Figure 4.2, the PVA/CNT/H_3PO_4 composite electrolytes can be observed from 0.1% CNT to 2% CNT, in 4.2.a through 4.2.d respectively. SEM images of the electrolytes in full resolution can be found in Appendix A. Upon visual inspection of the images, the carbon particles can be observed. In smaller weight percentages, there was less agglomeration and more uniform dispersion. However, as the weight percentage of CNT increased, larger clumps of carbon nanotubes could be seen because of poor solubility. In Figure 4.2.d, which is the 2% CNT, larger particles can be seen like the clump of particles pointed at by the orange arrow.

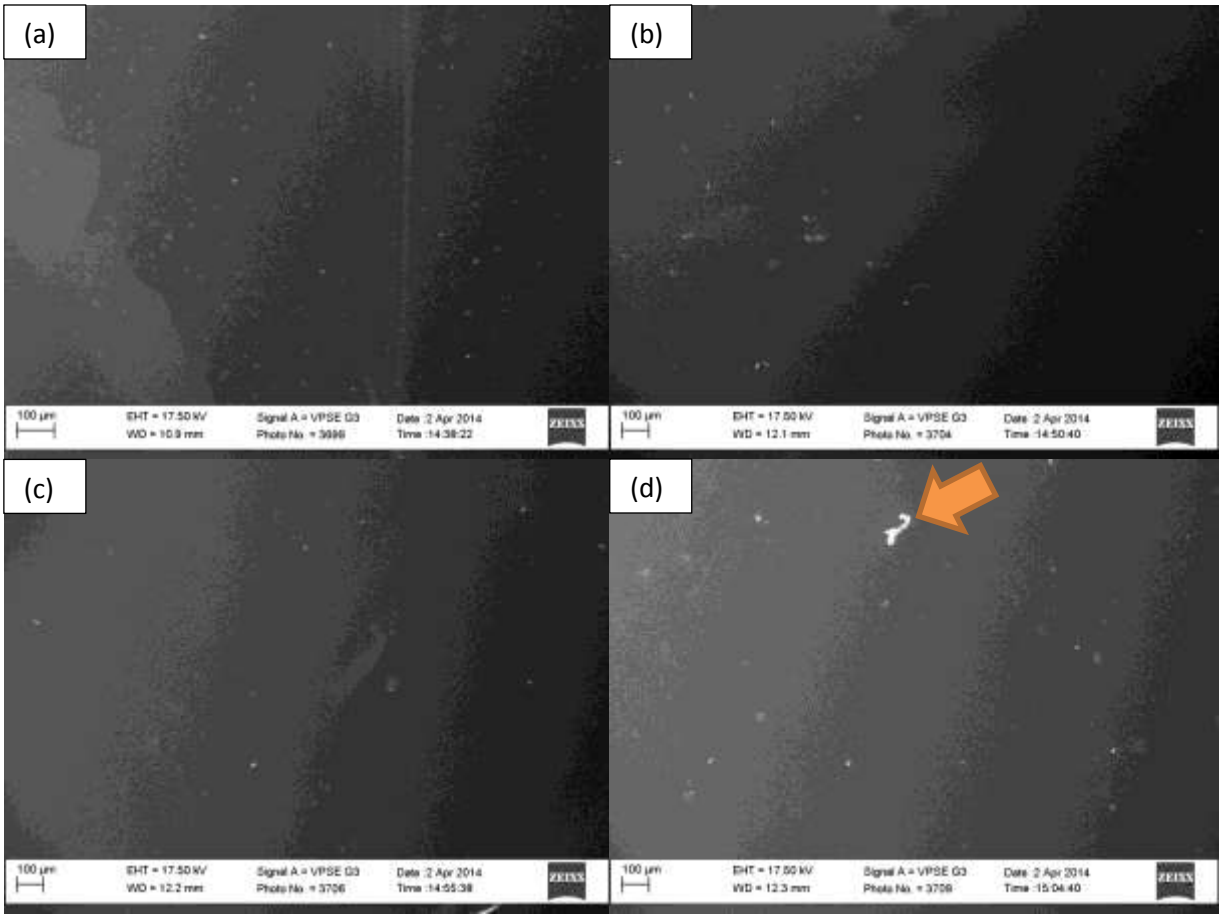

Figure 4.2 – SEM images of (a) 0.1% CNT (b) 0.5% CNT (c) 1%CNT and (d) 2% CNT.

4.2. Cyclic Voltammetry

Ideal capacitive behavior appears as a rectangular shape on a cyclic voltammogram [24]. However, under real conditions capacitors exhibit a parallelogram or a similar shape. Cyclic voltammograms for the baseline electrolyte with PVA and the electrolyte with 1% CNT addition can be seen in Figure 4.3. The graphs confirm capacitive behavior with rectangle-like shape. Full sized cyclic voltammogram graphs of every sample used in the experiment can be found in Appendix B.

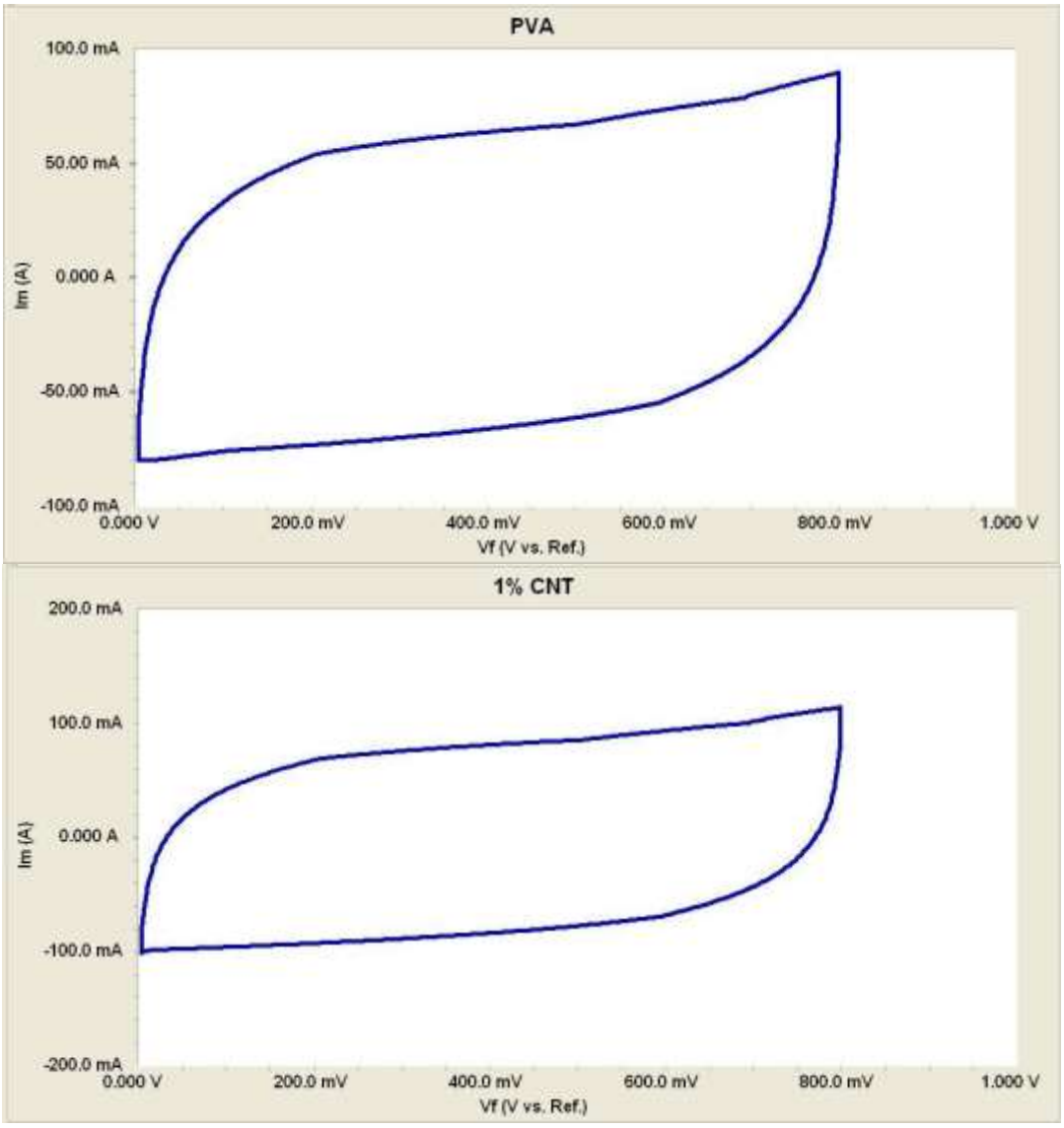

Figure 4.3 – Cyclic Voltammograms of (a) PVA/H_3PO_4 and (b) PVA/1%CNT/H_3PO_4.

Also, the capacitance can be obtained with cyclic voltammetry. Since the y-axis displays the current and the x-axis displays potential, the area underneath the curve will give the amount of charge stored. Therefore, capacitance can be calculated with the following equation [3]:

$$C = \frac{dQ}{dE} = \left|\frac{Q}{E_2 - E_1}\right| \quad (7)$$

The charge acummulated, Q, can be measured by the area of the CV graph between a potential window. By dividing the area by the potential window it covers (E_2-E_1) capacitance C was calculated. In Figure 4.4, the charge stored in the samples used in Figure 4.3 was calculated with Gamry EChem Analyst software.

Figure 4.4 – Calculating the charge accumulated in (a) PVA/H_3PO_4 and (b) PVA/1%CNT/H_3PO_4.

The charge accumulated for each supercapacitor was calculated between the 0V and 0.8V window for consistency since higher results could be obtained in different voltage windows. Using the capacitance equation, the following capacitances were found:

$$C_{(PVA)} = \frac{dQ}{dE} = \left|\frac{Q}{E_2 - E_1}\right| = \frac{0.4669C}{0.8V - 0V} = 0.584F$$

$$C_{(1\%)} = \frac{0.5929C}{0.8V - 0V} = 0.741F$$

However, capacitance value is not enough to determine performance since the size and weight of the capacitors greatly influence this value. Therefore, specific capacitance, which is the capacitance per unit mass of a material, was calculated by the following equation:

$$C_{s(PVA)} = \frac{C_{(PVA)}}{A}\frac{A}{m} = \frac{C_{(PVA)}}{m} = \frac{0.584F}{0.006g} = 97.27Fg^{-1}$$

$$C_{s(1\%)} = \frac{C_{(1\%)}}{m} = \frac{0.741F}{0.006g} = 123.52Fg^{-1}$$

The calculations for each supercapacitor were done in detail and can be found in Appendix C. Table 4.1 shows the results obtained for each supercapacitor and Figure 4.5 shows the relationship between the specific capacitance values. Since the PVA/H_3PO_4 electrolyte was the starting point to improve on, the percentage improvement of each supercapacitor in relation to it was also added to the table.

Table 4.1 – Specific capacitance results.

Supercapacitor (Electrolyte)	**Specific Capacitance (F/g)**	**% Improvement in Capacitance from PVA/H_3PO_4**
$PVA + H_3PO_4$	97.27	-
$PVA + 0.1\%\ CNT + H_3PO_4$	101.65	4.50
$PVA + 0.5\%\ CNT + H_3PO_4$	107.96	10.99
$PVA + 1\%\ CNT + H_3PO_4$	123.52	26.99
$PVA + 2\%\ CNT + H_3PO_4$	97.98	0.73

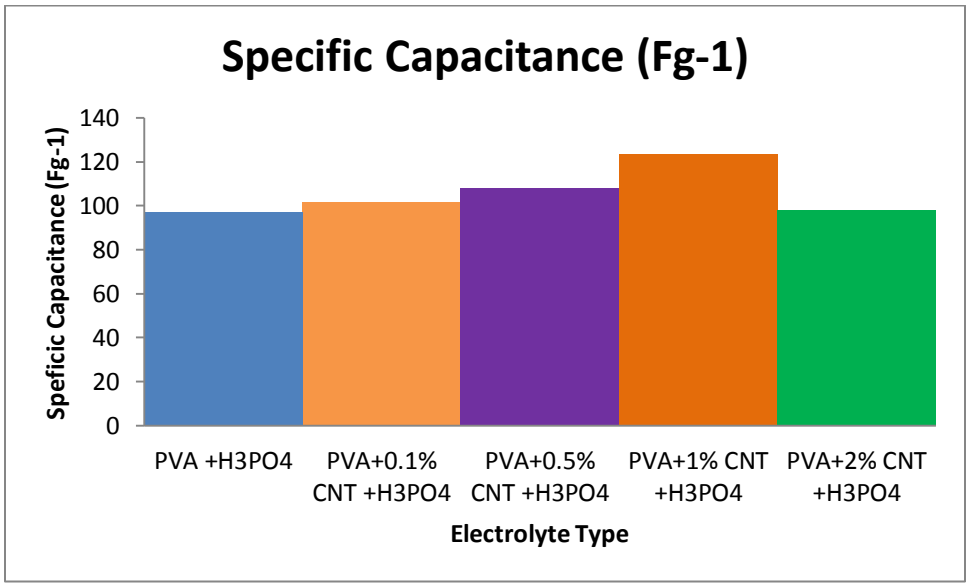

Figure 4.5 – Specific capacitance as a function of CNT in electrolyte.

The PVA/H_3PO_4 supercapacitor exhibited a specific capacitance of 97.27 Fg^{-1}, which is a similar result for a supercapacitor of this type [47]. Addition of CNT between 0.1 % and 1% improved specific capacitance a great deal. Addition of 0.5% CNT increased the specific

capacitance up to 107.96 Fg^{-1}, and addition of 1% CNT achieved 123.52 Fg^{-1}, which is a staggering 27% increase in capacitance. Compared previously made solid-state supercapacitors with PVA electrolytes and their specific capacitance values between 90.83 Fg^{-1} and 105.78 Fg^{-1} [47], 0.5% and 1% CNT supercapacitors definitely show an improvement. Although the 2% CNT exhibited a higher capacitance value, it is too small of an increase to show as a significant improvement. This could be attributed to the agglomerations occurring in the electrolyte, causing imperfections on the surface and gaps between the electrodes.

4.3. Electrolyte Resistivity

Since the scope of the experiments revolved around electrolytes, it was beneficial to inspect the resistivity values. The extra electrolyte films constructed during the production of the supercapacitors were used to measure resistivity. The 2x2 cm electrolytes were used for measurements. Though an effort was made to make films with similar thickness, the values varied. The calculations can be found in Appendix D.

Table 4.2 – The electrolyte resistivity values.

Electrolytes	**Resistivity (Ωcm)**	**Thickness (cm)**
PVA +H_3PO_4	$3.97x10^2$	0.0124
PVA+0.1% CNT +H_3PO_4	$3.87x10^2$	0.0149
PVA+0.5% CNT +H_3PO_4	$2.94x10^2$	0.0070
PVA+1% CNT +H_3PO_4	$3.06x10^2$	0.0075
PVA+2% CNT +H_3PO_4	$3.31x10^2$	0.0077

Predictably, a similar trend to capacitance values is exhibited in electrolyte resistivity. PVA/H_3PO_4 sheet exhibited the highest resistivity of 397 Ωcm, and the addition of CNT improved the measurements by reducing the resistivity. The lowest resistivity was exhibited by 0.5% CNT at 294 Ωcm. 1% CNT with the highest capacitance had the second best value at 306 Ωcm. These values fall short of organic electrolytes, which exhibit resistivity values around 20-60 Ωcm [9]. However, since supercapacitors with organic electrolytes cannot be used in certain applications that require no liquid components, the solid electrolytes still prove to be promising.

4.4. Charge/Discharge Behavior

The charging and discharging of the supercapacitors were observed with the oscilloscope, which plots the voltage potential of the cell versus time. The potential vs. time graph of PVA electrolyte with no CNT added is pictured in Figure 4.6, and the graph for 1% CNT is pictured in Figure 4.7. These two supercapacitors were used as the examples since PVA electrolyte was the baseline, and the 1% CNT because it showed the best performance in other categories.

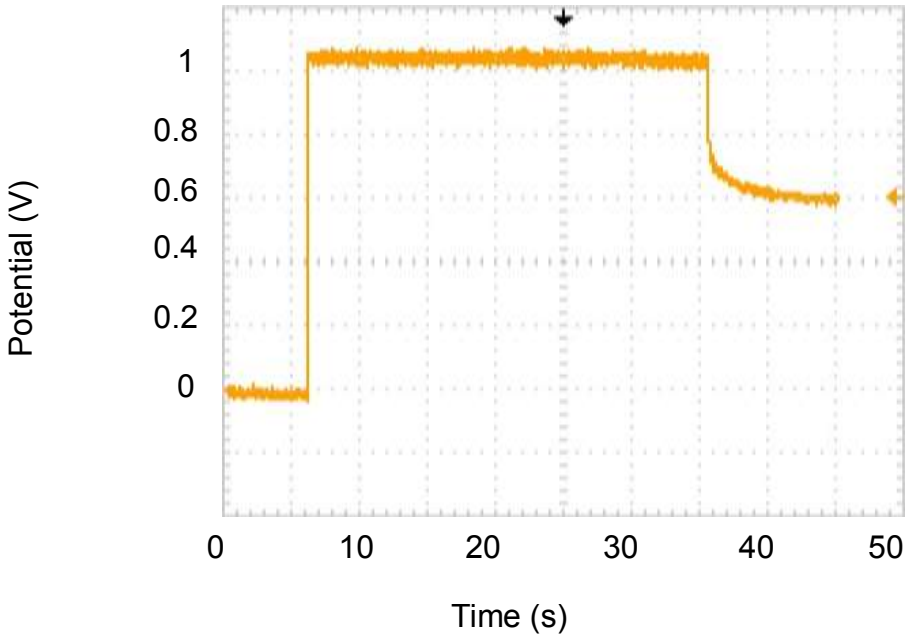

Figure 4.6 – Potential vs. time curve for supercapacitor with PVA electrolyte.

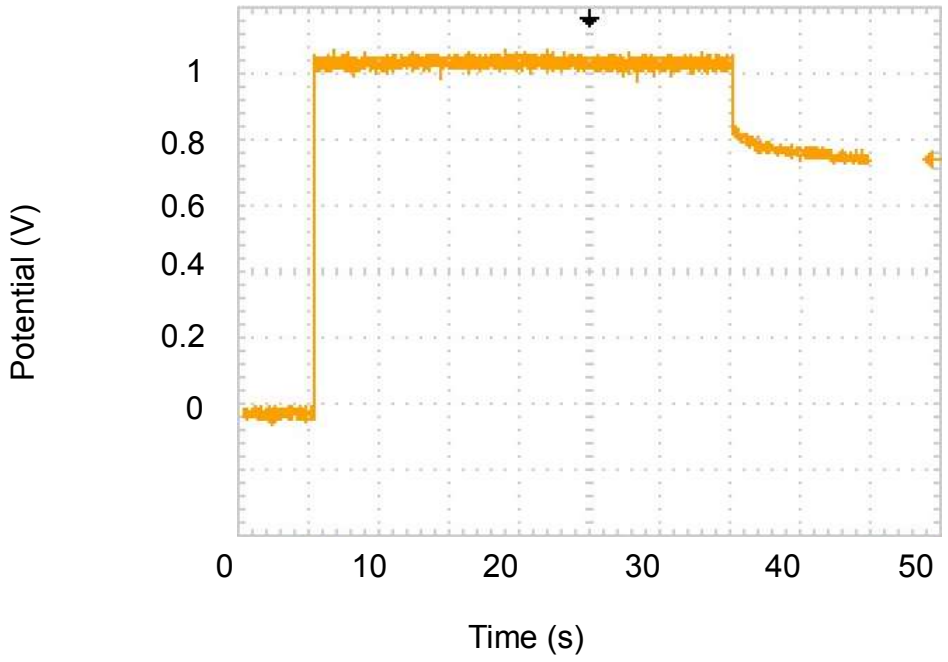

Figure 4.7 – Potential vs. time curve for supercapacitor with 1% CNT electrolyte.

Both supercapacitors were charged for 30 seconds with 1 V direct current. After 30 seconds, the power supply was cut off and the resulting discharge curve was observed. In both samples, an immediate voltage drop was observed. This drop was attributed to the internal resistance and the lower drop in 1% CNT confirmed that. The discharge rates were effectively in line with each other since the circuit setup was same for both experiments. Different discharge curve slopes could appear with the introduction of another resistor into the circuit. Overall, both samples exhibited typical supercapacitor charge/discharge behavior.

CHAPTER 5

CONCLUSION AND FUTURE WORK

5.1. Conclusion

In this thesis, improvement methods on solid-state supercapacitors were examined. This study focused on the electrolytes since it is the component that determines whether a supercapacitor is exclusively solid-state. PVA/H_3PO_4 electrolyte was chosen to construct the supercapacitor because of its environmental friendliness, simple production, relatively low cost, high safety, and other promising properties that could still be improved. CNT was added to the PVA in order to create a composite electrolyte matrix that demonstrates better electrical properties, while retaining the environmental and safety aspects of pure PVA. Carbon nanotubes were chosen for their good electrical and mechanical properties, as well as their ability to be dispersed in PVA solution.

Scanning electron microscopy, cyclic voltammetry, and resistivity measurements were all performed on the electrodes and electrolytes. Also, charging and discharging behavior of the supercapacitors were inspected. Taking the results of these experiments into consideration, PVA/CNT nanocomposites could be used to improve solid electrolyte performance. 1wt% CNT yielded the best results with a specific capacitance of 123.52 Fg^{-1}, a 27% improvement from no CNT present. 1wt% CNT also exhibited an electrolyte resistivity of 306 Ωcm, which greatly affects the power density of the supercapacitor. 0.5% CNT also exhibited impressive results with a specific capacitance of 107.96 Fg^{-1} and an electrolyte resistivity of 294 Ωcm, which was the lowest of all. The slight increased resistance in the 1% CNT is outweighed by the increase in specific capacitance, making the 1.0wt% CNT an overall better electrolyte than the 0.5wt%.

However, the 2wt% CNT barely showed any improvement at all on the 1% electrolyte. This was attributed to the lack of solubility of CNT past a 1wt% concentration. Therefore, it could be concluded that CNT addition to a solid PVA electrolyte improves electrical properties up to a point where excess CNT becomes insoluble.

Although solid-state supercapacitors do not exhibit liquid supercapacitor performance, with their unique properties, they will prove useful in niche applications. They would be particularly useful in products where liquid storage is inconvenient or detrimental. In addition, the ultra-thin supercapacitors can be made in any shape and size, a valuable property for slim electronic devices. The flexibility and portability of the supercapacitors is unparalleled in energy storage, making them a front-runner in developing markets like wearable electronics. They are the safer, environmentally friendlier alternative to batteries and capacitors with liquid components. Their production could be easily scaled up without major cost increases or assembly challenges. These experiments have led to improvements in solid-state supercapacitors, increasing their promise in future applications.

5.2. Future Work

Supercapacitor technology is growing rapidly and opening doors for new applications. Solid-state supercapacitors have a lot of promising applications such as wearable electronics, but also a lot of room for improvement. A more detailed study should be done on CNT/PVA composite electrolytes, especially a study that focuses on the voltage factors. A test to determine the maximum operating voltage with a long life cycle will be beneficial in order to be able to improve the energy density. A variety of carbons, like carbon black and graphene, could be incorporated into polymer composites in order to create solid electrolytes with great electrical properties. The different carbon materials could be combined in the same electrolyte as well,

varying their relative concentrations. By combining PVA with two types of carbon, both with different electrical and mechanical properties, might yield impressive results. Experiments could also be conducted with CNT and polymers other than PVA. The different physical properties of the polymers could add additional strength or stiffness to the supercapacitor, if such properties are needed for a specific application.

In addition to studying changes in the electrolyte, the properties of the electrodes could also be modified. For example, testing could be done after changing the carbon material or adding another conductive component to the graphene oxide before reduction. The electrodes could be synthesized with different binding surfaces, allowing for more or less flexibility. Even varying the thickness of the electrolyte between the electrodes could cause changes in resistance and specific capacitance, possibly leading to an ideal width and composition.

REFERENCES

[1] Sharma, P., & Bhatti, T. S. (2010). A review on electrochemical double-layer capacitors. *Energy Conversion and Management*, *51*(12), 2901-2912.

[2] Christen, T., & Carlen, M. W. (2000). Theory of Ragone plots. *Journal of power sources*, *91*(2), 210-216.

[3] H. I. Becker. Low voltage electrolytic capacitor. United States Patent 2800616, 1957.

[4] Lu, Max. (2013). *Supercapacitors: Materials, Systems and Applications*. Eds. Francois Beguin, and Elzbieta Frackowiak. John Wiley & Sons.

[5]Wang, G., Zhang, L., & Zhang, J. (2012). A review of electrode materials for electrochemical supercapacitors. *Chemical Society Reviews*, *41*(2), 797-828.

[6] Simon, P., & Gogotsi, Y. (2008). Materials for electrochemical capacitors. *Nature materials*, *7*(11), 845-854.

[7] Frackowiak, E. (2007). Carbon materials for supercapacitor application. *Physical Chemistry Chemical Physics*, *9*(15), 1774-1785.

[8] Inagaki, M., Konno, H., & Tanaike, O. (2010). Carbon materials for electrochemical capacitors. *Journal of Power Sources*, *195*(24), 7880-7903.

[9] Burke, A. (2000). Ultracapacitors: why, how, and where is the technology. *Journal of power sources*, *91*(1), 37-50.

[10] The Science of Dispersion and Influencing Double Layer for Colloidal Dispersion Stability, Zeta West.. Retrieved 2014, from http://www.zetawest.com/science.html

[11] Belhachemi, F., Rael, S., & Davat, B. (2000). A physical based model of power electric double-layer supercapacitors. In *Industry Applications Conference, 2000. Conference Record of the 2000 IEEE* (Vol. 5, pp. 3069-3076). IEEE.

[12] Ryu, K. S., Kim, K. M., Park, Y. J., Park, N. G., Kang, M. G., & Chang, S. H. (2002). Redox supercapacitor using polyaniline doped with Li salt as electrode. *Solid State Ionics*, *152*, 861-866.

[13] Chuang, C. M., Huang, C. W., Teng, H., & Ting, J. M. (2010). Effects of carbon nanotube grafting on the performance of electric double layer capacitors. *Energy & Fuels*, *24*(12), 6476-6482.

[14] Frackowiak, E., & Beguin, F. (2001). Carbon materials for the electrochemical storage of energy in capacitors. *Carbon*, *39*(6), 937-950.

[15] Snook, G. A., Kao, P., & Best, A. S. (2011). Conducting-polymer-based supercapacitor devices and electrodes. *Journal of Power Sources*, *196*(1), 1-12.

[16] Lokhande, C. D., Dubal, D. P., & Joo, O. S. (2011). Metal oxide thin film based supercapacitors. *Current Applied Physics*, *11*(3), 255-270.

[17] Zhao, D. D., Bao, S. J., Zhou, W. J., & Li, H. L. (2007). Preparation of hexagonal nanoporous nickel hydroxide film and its application for electrochemical capacitor. *Electrochemistry communications*, *9*(5), 869-874.

[18] Zhou, Y. K., He, B. L., Zhou, W. J., Huang, J., Li, X. H., Wu, B., & Li, H. L. (2004). Electrochemical capacitance of well-coated single-walled carbon nanotube with polyaniline composites. *Electrochimica Acta*, *49*(2), 257-262.

[19] Fan, L. Z., Hu, Y. S., Maier, J., Adelhelm, P., Smarsly, B., & Antonietti, M. (2007). High electroactivity of polyaniline in supercapacitors by using a hierarchically porous carbon monolith as a support. *Advanced Functional Materials*, *17*(16), 3083-3087.

[20] Mastragostino, M., Arbizzani, C., & Soavi, F. (2002). Conducting polymers as electrode materials in supercapacitors. *Solid state ionics*, *148*(3), 493-498.

[21] Frackowiak, E., Khomenko, V., Jurewicz, K., Lota, K., & Beguin, F. (2006). Supercapacitors based on conducting polymers/nanotubes composites. *Journal of Power Sources*, *153*(2), 413-418

[22] Hashmi, S. A., & Upadhyaya, H. M. (2002). Polypyrrole and poly (3-methyl thiophene)-based solid state redox supercapacitors using ion conducting polymer electrolyte. *Solid State Ionics*, *152*, 883-889.

[23] Ryu, K. S., Kim, K. M., Park, N. G., Park, Y. J., & Chang, S. H. (2002). Symmetric redox supercapacitor with conducting polyaniline electrodes. *Journal of Power Sources*, *103*(2), 305-309.

[24] Vol'fkovich, Y. M., & Serdyuk, T. M. (2002). Electrochemical capacitors. *Russian journal of electrochemistry*, *38*(9), 935-959.

[25] Sivakkumar, S. R., & Saraswathi, R. (2004). Performance evaluation of poly (< i> N</i>-methylaniline) and polyisothianaphthene in charge-storage devices. *Journal of power sources*, *137*(2), 322-328.

[26] Inagaki, M., Konno, H., & Tanaike, O. (2010). Carbon materials for electrochemical capacitors. *Journal of Power Sources*, *195*(24), 7880-7903.

[27] Zhang, Y., Feng, H., Wu, X., Wang, L., Zhang, A., Xia, T., ... & Zhang, L. (2009). Progress of electrochemical capacitor electrode materials: A review. *International journal of hydrogen energy*, *34*(11), 4889-4899.

[28] Largeot, C., Portet, C., Chmiola, J., Taberna, P. L., Gogotsi, Y., & Simon, P. (2008). Relation between the ion size and pore size for an electric double-layer capacitor. *Journal of the American Chemical Society*, *130*(9), 2730-2731.

[29] Kötz, R., & Carlen, M. (2000). Principles and applications of electrochemical capacitors. *Electrochimica Acta*, *45*(15), 2483-2498.

[30] Huang, Y., Liang, J., & Chen, Y. (2012). An Overview of the Applications of Graphene-Based Materials in Supercapacitors. *Small*, *8*(12), 1805-1834.

[31] Si, Y., & Samulski, E. T. (2008). Exfoliated graphene separated by platinum nanoparticles. *Chemistry of Materials*, *20*(21), 6792-6797.

[32] Hummers Jr, W. S., & Offeman, R. E. (1958). Preparation of graphitic oxide. *Journal of the American Chemical Society*, *80*(6), 1339-1339.

[33] Kovtyukhova, N. I., Ollivier, P. J., Martin, B. R., Mallouk, T. E., Chizhik, S. A., Buzaneva, E. V., & Gorchinskiy, A. D. (1999). Layer-by-layer assembly of ultrathin composite films from micron-sized graphite oxide sheets and polycations. *Chemistry of Materials*, *11*(3), 771-778.

[34] Stankovich, S., Dikin, D. A., Piner, R. D., Kohlhaas, K. A., Kleinhammes, A., Jia, Y., ... & Ruoff, R. S. (2007). Synthesis of graphene-based nanosheets via chemical reduction of exfoliated graphite oxide. *Carbon*, *45*(7), 1558-1565.

[35] Chen, Y., Zhang, X., Zhang, D., Yu, P., & Ma, Y. (2011). High performance supercapacitors based on reduced graphene oxide in aqueous and ionic liquid electrolytes. *Carbon*, *49*(2), 573-580.

[36] McAllister, M. J., Li, J. L., Adamson, D. H., Schniepp, H. C., Abdala, A. A., Liu, J., ... & Aksay, I. A. (2007). Single sheet functionalized graphene by oxidation and thermal expansion of graphite. *Chemistry of Materials*, *19*(18), 4396-4404.

[37] Schniepp, H. C., Li, J. L., McAllister, M. J., Sai, H., Herrera-Alonso, M., Adamson, D. H., ... & Aksay, I. A. (2006). Functionalized single graphene sheets derived from splitting graphite oxide. *The Journal of Physical Chemistry B*, *110*(17), 8535-8539.

[38] Vivekchand, S. R. C., Rout, C. S., Subrahmanyam, K. S., Govindaraj, A., & Rao, C. N. R. (2008). Graphene-based electrochemical supercapacitors. *Journal of Chemical Sciences*, *120*(1), 9-13.

[39] Li, Y., Gao, W., Ci, L., Wang, C., & Ajayan, P. M. (2010). Catalytic performance of Pt nanoparticles on reduced graphene oxide for methanol electro-oxidation. *Carbon*, *48*(4), 1124-1130.

[40] Seger, B., & Kamat, P. V. (2009). Electrocatalytically active graphene-platinum nanocomposites. Role of 2-D carbon support in PEM fuel cells. *The Journal of Physical Chemistry C*, *113*(19), 7990-7995.

[41] Qiu, J. D., Wang, G. C., Liang, R. P., Xia, X. H., & Yu, H. W. (2011). Controllable deposition of platinum nanoparticles on graphene as an electrocatalyst for direct methanol fuel cells. *The Journal of Physical Chemistry C*, *115*(31), 15639-15645.

[42] El-Kady, M. F., Strong, V., Dubin, S., & Kaner, R. B. (2012). Laser scribing of high-performance and flexible graphene-based electrochemical capacitors. *Science*, *335*(6074), 1326-1330.

[43] Khomenko, V., Raymundo-Piñero, E., & Béguin, F. (2008). High-energy density graphite/AC capacitor in organic electrolyte. *Journal of Power Sources*, *177*(2), 643-651.

[44] Galiński, M., Lewandowski, A., & Stępniak, I. (2006). Ionic liquids as electrolytes. *Electrochimica Acta*, *51*(26), 5567-5580.

[45] Wang, Y. G., & Zhang, X. G. (2004). All solid-state supercapacitor with phosphotungstic acid as the proton-conducting electrolyte. Solid State Ionics, 166(1), 61-67.

[46] Yuan, L., Lu, X. H., Xiao, X., Zhai, T., Dai, J., Zhang, F., ... & Wang, Z. L. (2011). Flexible solid-state supercapacitors based on carbon nanoparticles/MnO2 nanorods hybrid structure. *Acs Nano*, *6*(1), 656-661.

[47] Yang, C. C., Hsu, S. T., & Chien, W. C. (2005). All solid-state electric double-layer capacitors based on alkaline polyvinyl alcohol polymer electrolytes. *Journal of power sources*, *152*, 303-310.

[48] Schneuwly, A., & Gallay, R. (2000). Properties and applications of supercapacitors: From the state-of-the-art to future trends. *Rossens, Switzerland*.

[49] Yu, H., Tang, Q., Wu, J., Lin, Y., Fan, L., Huang, M., ... & Yu, F. (2012). Using eggshell membrane as a separator in supercapacitor. *Journal of Power Sources*, *206*, 463-468.

[50] *Cars, trucks, buses, and "nonroad" equipment*. (2012, March 6). Retrieved 2014, from http://www.epa.gov/air/caa/peg/carstrucks.html

[51] Kötz, R., Bärtschi, M., Büchi, F., Gallay, R., & Dietrich, P. (2002, December). HY. POWER–A fuel cell car boosted with supercapacitors. In *Proc. of the 12th International Seminar on Double Layer Capacitors and Similar Energy Storage Devices, Deerfield Beach, FL*.

[52] Kötz, R., Müller, S., Bärtschi, M., Schnyder, B., Dietrich, P., Büchi, F. N., ... & Gallay, R. (2001, September). Supercapacitors for peak-power demand in fuel-cell-driven cars. In *ECS Electro-Chemical Society, 52nd Meeting,, San Francisco*.

[53] Spillane, D., O'sullivan, D., Egan, M. G., & Hayes, J. G. (2003, February). Supervisory control of a HV integrated starter-alternator with ultracapacitor support within the 42 V automotive electrical system. In *Applied Power Electronics Conference and Exposition, 2003. APEC'03. Eighteenth Annual IEEE* (Vol. 2, pp. 1111-1117). IEEE.

[54] Mithulananthan, N., Canizares, C. A., Reeve, J., & Rogers, G. J. (2003). Comparison of PSS, SVC, and STATCOM controllers for damping power system oscillations. *Power Systems, IEEE Transactions on*, *18*(2), 786-792.

[55] Hingorani, N. G. (1995). Introducing custom power. *Spectrum, IEEE*, *32*(6), 41-48.

[56] Andrieu, X., & Fauvarque, J. F. (1993, September). Supercapacitors for telecommunication applications. In *Telecommunications Energy Conference, INTELEC'93. 15th International* (Vol. 1, pp. 79-82). IEEE.

[57] Barker, P. P. (2002, July). Ultracapacitors for use in power quality and distributed resource applications. In *Power Engineering Society Summer Meeting, 2002 IEEE* (Vol. 1, pp. 316-320). IEEE.

[58] Merryman, S. A. (1996, August). Chemical double-layer capacitor power sources for electrical actuation applications. In *Energy Conversion Engineering Conference, 1996. IECEC 96., Proceedings of the 31st Intersociety* (Vol. 1, pp. 251-254). IEEE.

[59] Merryman, S. A., & Hall, D. K. (1997). Characterization of CDL capacitor power sources for electrical actuation applications. In *Energy Conversion Engineering Conference, 1997. IECEC-97., Proceedings of the 32nd Intersociety* (Vol. 1, pp. 297-301). IEEE.

[60] Robbins, T., & Hawkins, J. M. (1997, October). Powering telecommunications network interfaces using photovoltaic cells and supercapacitors. In *Telecommunications Energy Conference, 1997. INTELEC 97., 19th International* (pp. 523-528). IEEE.

[61] Thounthong, P., Chunkag, V., Sethakul, P., Sikkabut, S., Pierfederici, S., & Davat, B. (2011). Energy management of fuel cell/solar cell/supercapacitor hybrid power source. *Journal of Power Sources*, *196*(1), 313-324.

[62] Geim, A. K., Novoselov, K. S., Yazyev, O. V., Louie, S. G., Ghosh, S., Bao, W., ... & Rotenberg, E. (2007). Nobel Prize for graphene. *Nature Materials*, *6*, 183-192.

[63] Geim, A. K., & Novoselov, K. S. (2007). The rise of graphene. *Nature materials*, *6*(3), 183-191.

[64] Neto, A. C., Guinea, F., Peres, N. M. R., Novoselov, K. S., & Geim, A. K. (2009). The electronic properties of graphene. *Reviews of modern physics*, *81*(1), 109.

[65] Novoselov, K. S., Geim, A. K., Morozov, S. V., Jiang, D., Zhang, Y., Dubonos, S. V., ... & Firsov, A. A. (2004). Electric field effect in atomically thin carbon films. *science*, *306*(5696), 666-669.

[66] Iijima, S. (1991). Helical microtubules of graphitic carbon. *nature*, *354*(6348), 56-58.

[67] Khare, R., & Bose, S. (2005). Carbon nanotube based composites-a review. *Journal of minerals and Materials Characterization and Engineering*, *4*, 31.

[68] Paradise, M., & Goswami, T. (2007). Carbon nanotubes–production and industrial applications. *Materials & Design*, *28*(5), 1477-1489.

[69] Yamabe, T. (1995). Recent development of carbon nanotube. *Synthetic Metals*, *70*(1), 1511-1518.

[70] Hong, S., & Myung, S. (2007). A flexible approach to mobility. *Nature Nanotech*, *2*, 207-208.

[71] Asmatulu, R. (Ed.). (2013). *Nanotechnology Safety*. Elsevier, The Nederland.

[72] *Harrick Plasma: Plasma cleaning: Applications*. (2013). Retrieved 2014, from http://www.harrickplasma.com/applications_cleaning.php

[73] Anderson, D. E., Gore, M. P., & McClellan, P. J. (2007). Integrated CD/DVD recording and labeling.

[74] Jiang, L., Vangari, M., Pryor, T., Xiao, Z., & Korivi, N. S. (2013). Miniature supercapacitors based on nanocomposite thin films. *Microelectronic Engineering*, *111*, 52-57.

[75] "Cyclic voltammetry." *Journal of Chemical Education* 60, no. 9 (1983): 702.

[76] "Electrochemical Energy » Gamry Instruments." Retrieved 2014, from http://www.gamry.com/application-notes/energy/

[77] Gamry Instruments. “Gamry Reference 600 Potentiostat/Galvanostat/ZRA Operator’s Manual.” (2012).

APPENDICES

Appendix A – SEM Images

Graphene Oxide

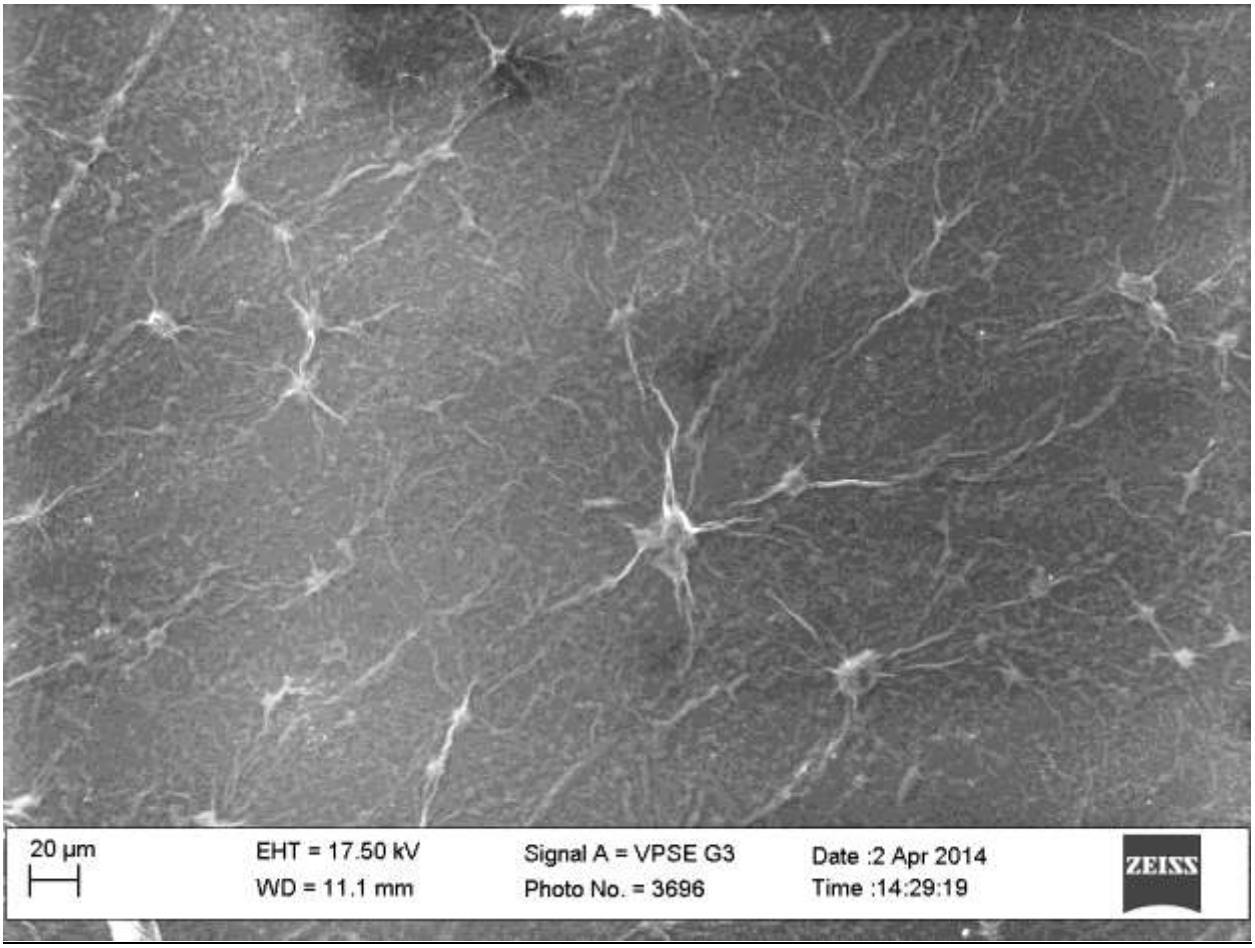

Graphene Oxide (+Magnification)

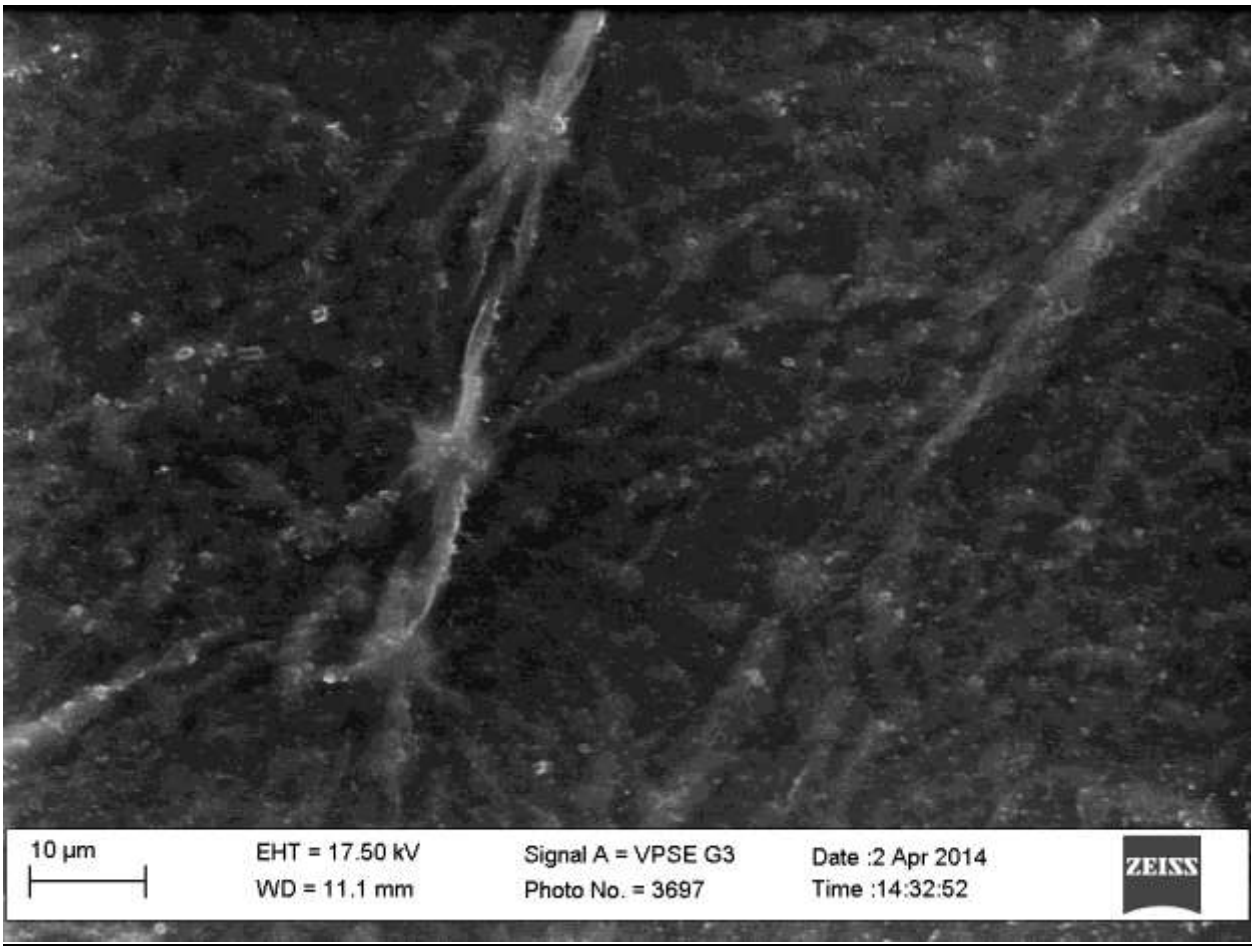

Laser Reduced Graphene

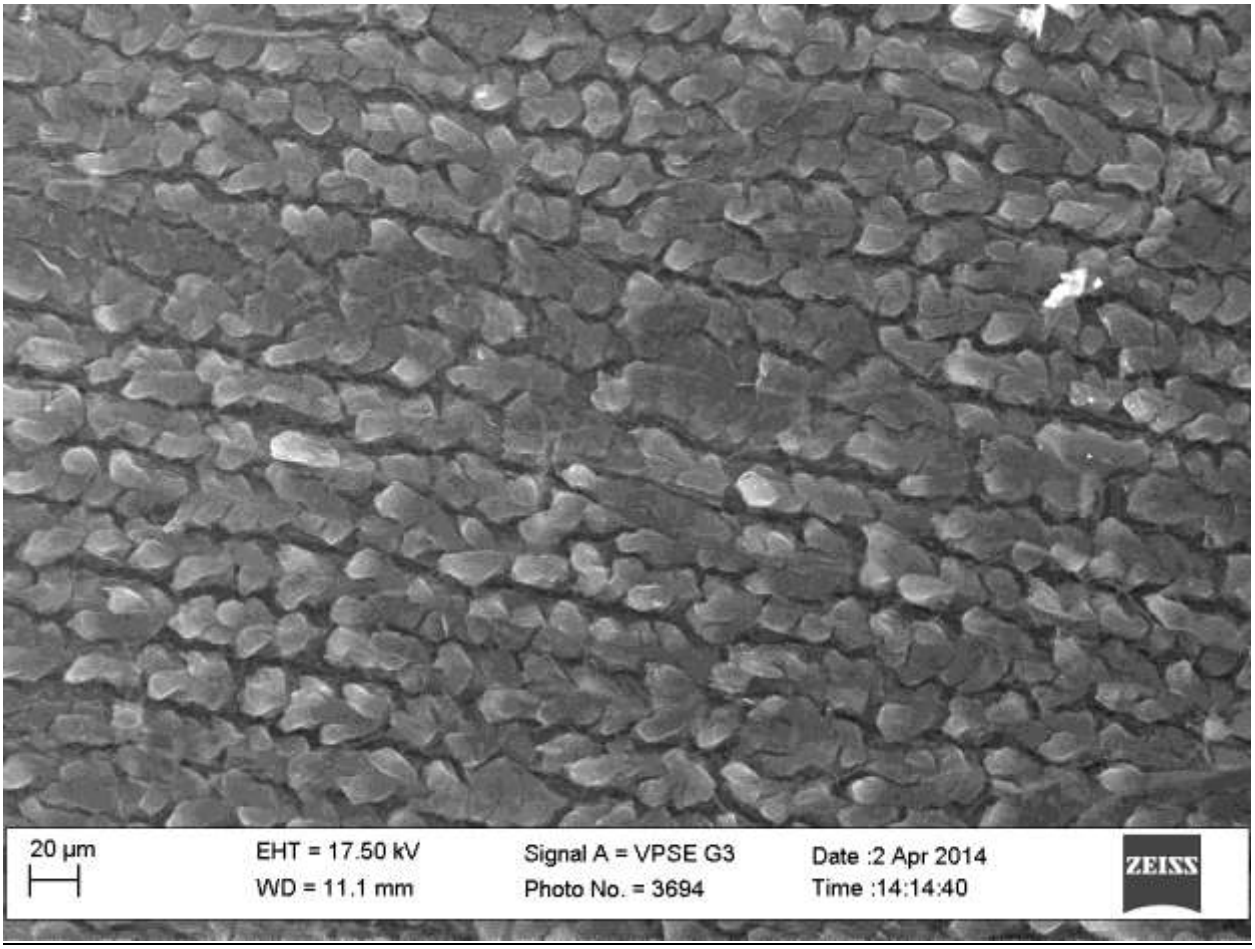

Laser Reduced Graphene (+Magnification)

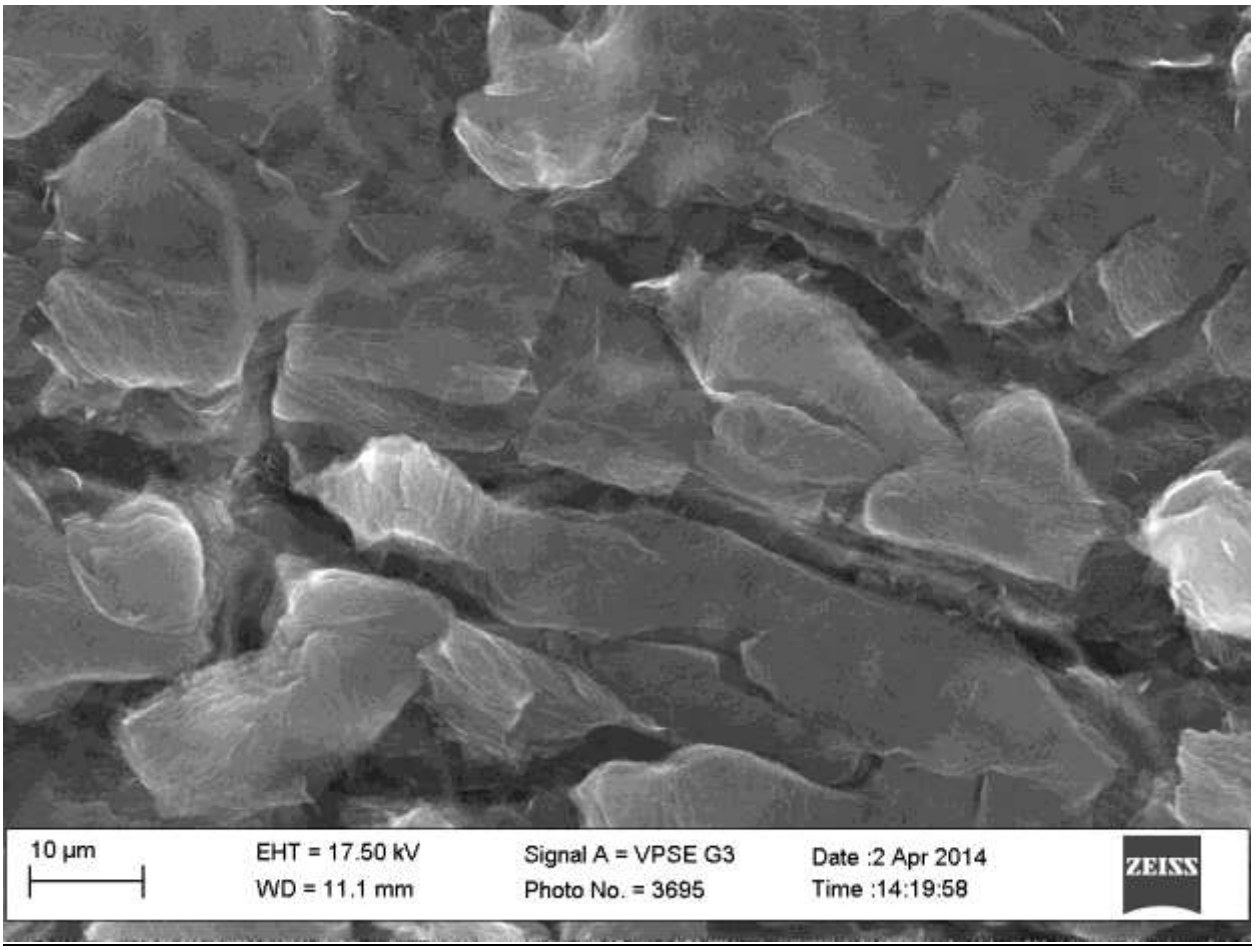

0.1% CNT Electrolyte

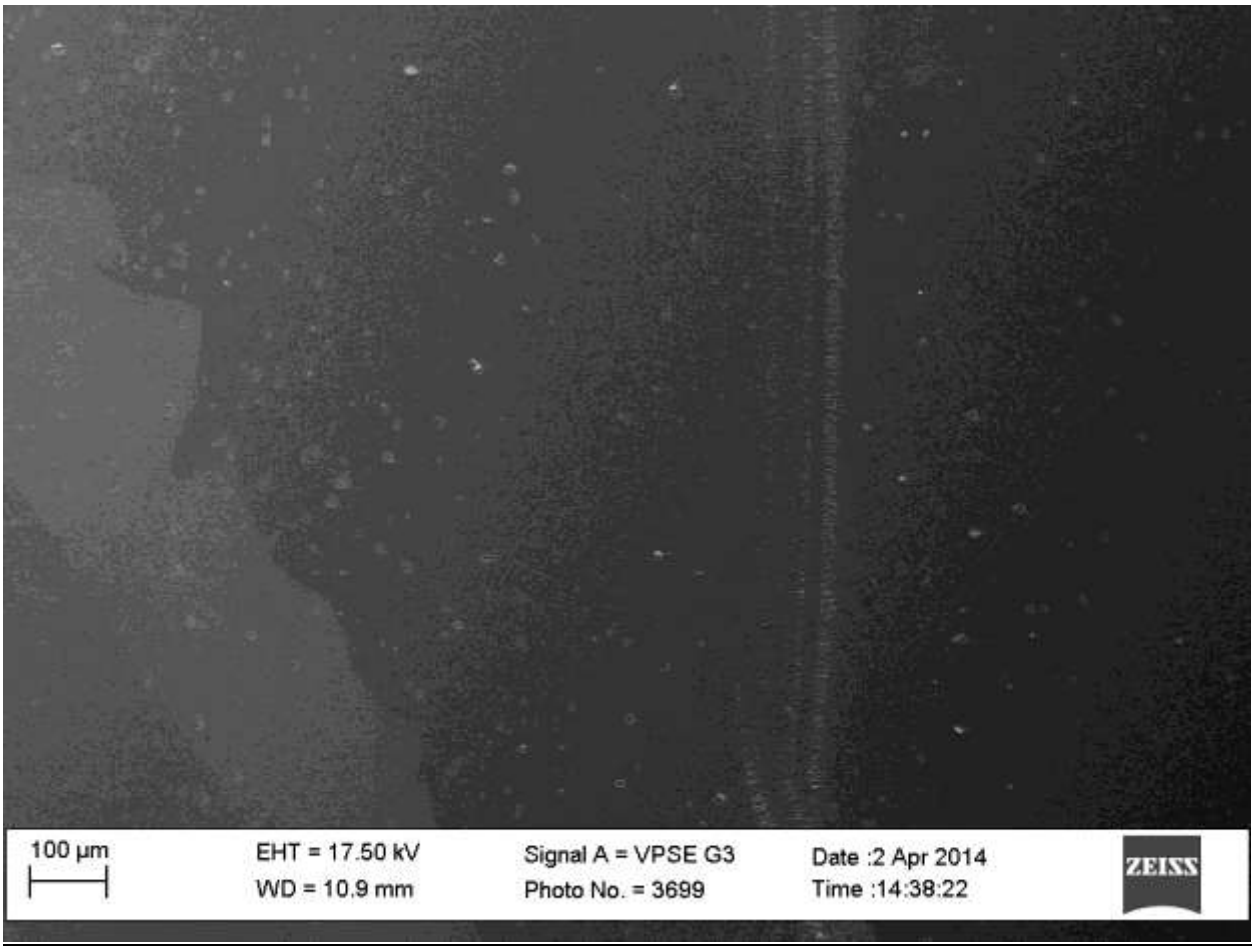

0.5% CNT Electrolyte

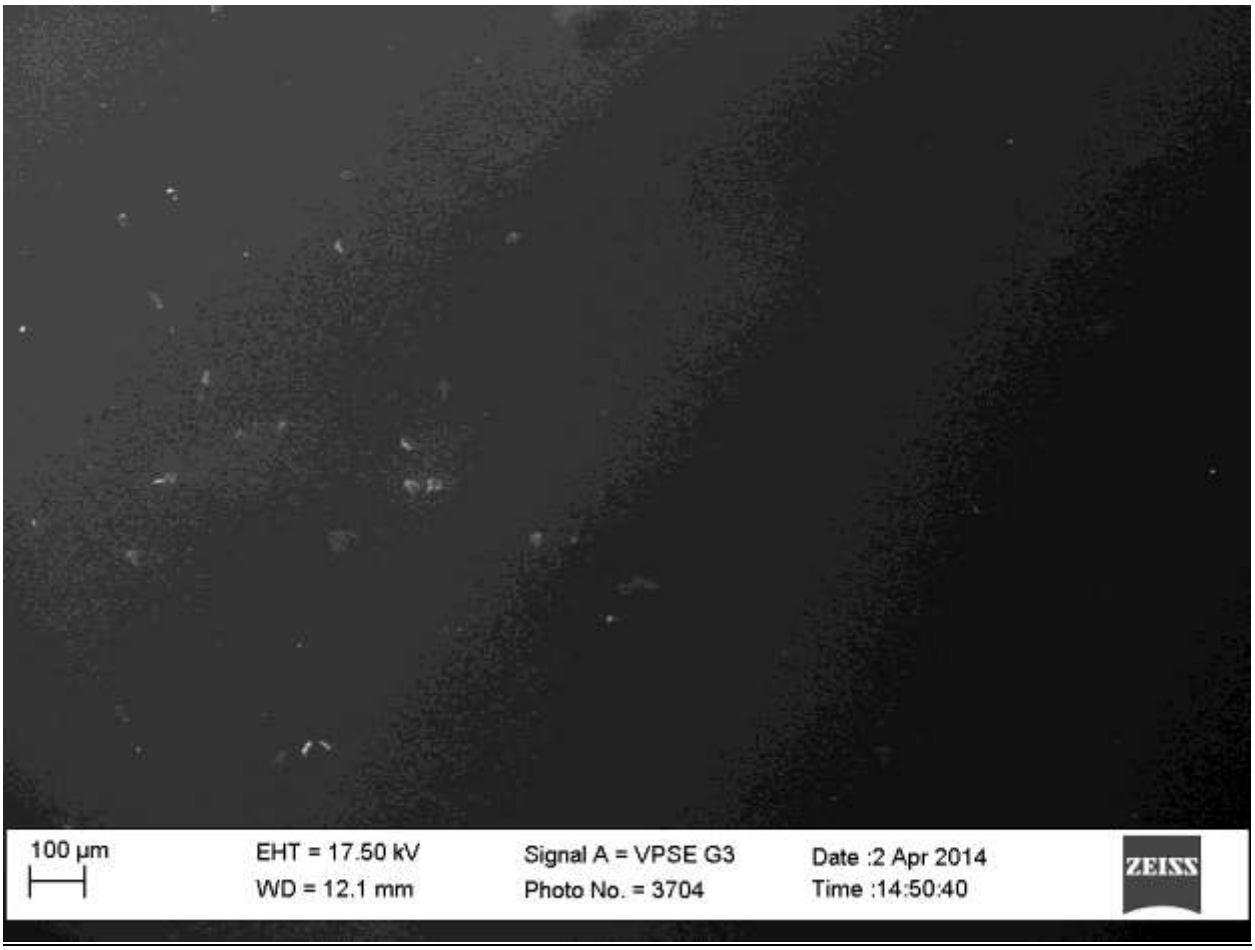

1% CNT Electrolyte

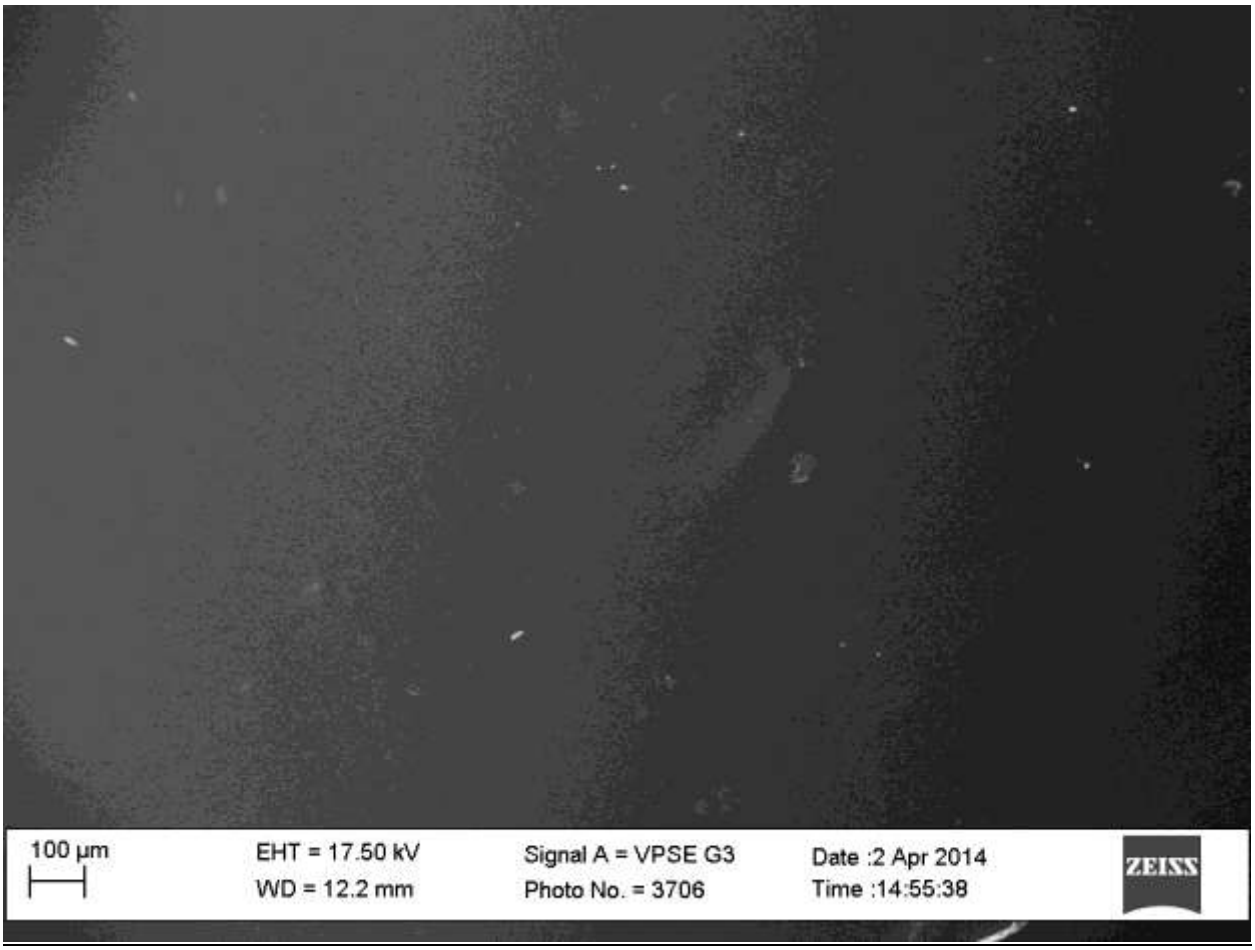

2% CNT Electrolyte

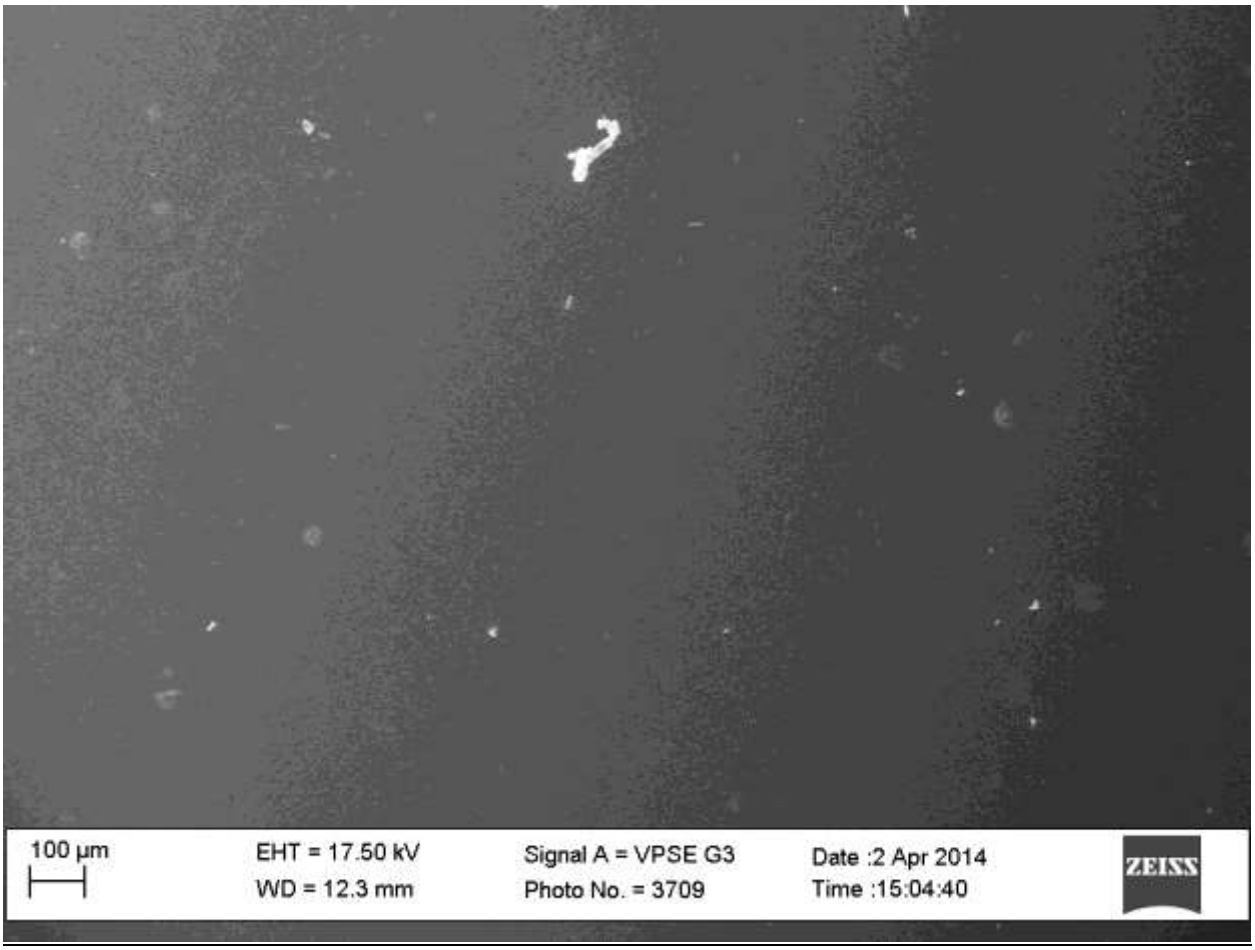

Appendix B – Cyclic Voltammograms

No CNT Added

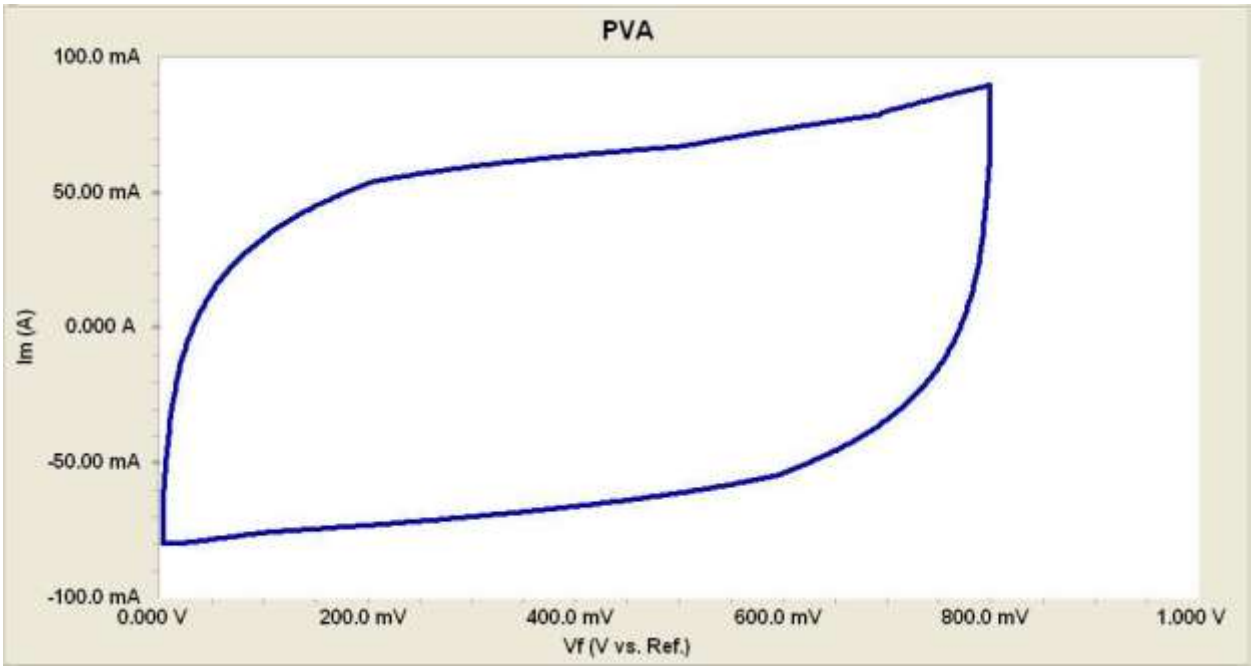

0.1% CNT

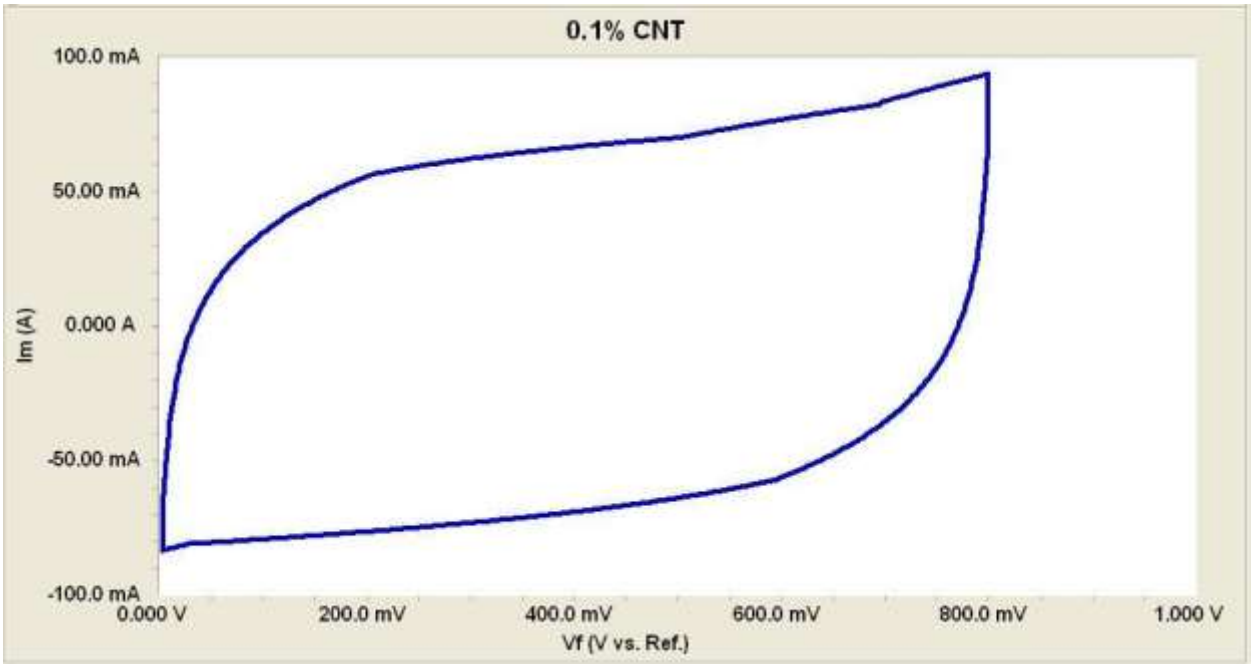

0.5% CNT

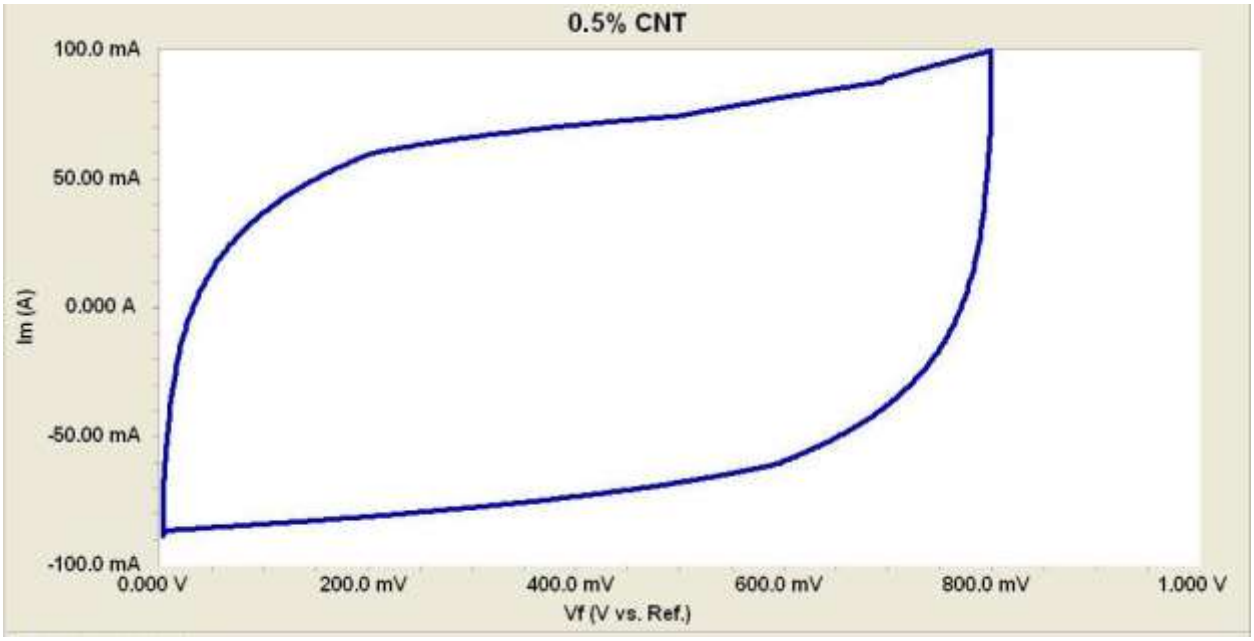
0.5% CNT
100.0 mA
50.00 mA
0.000 A
-50.00 mA
-100.0 mA
Im (A)
0.000 V
200.0 mV
400.0 mV
600.0 mV
800.0 mV
1.000 V
Vf (V vs. Ref.)

1% CNT

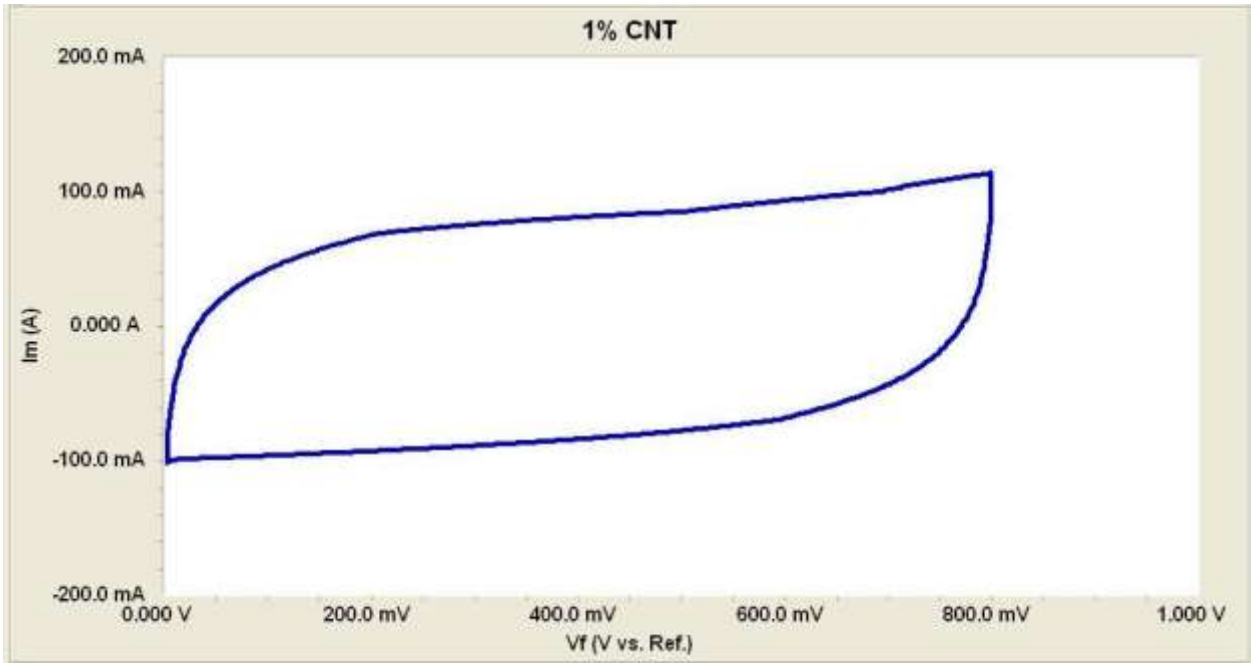
1% CNT
200.0 mA
100.0 mA
0.000 A
-100.0 mA
-200.0 mA
Im (A)
0.000 V
200.0 mV
400.0 mV
600.0 mV
800.0 mV
1.000 V
Vf (V vs. Ref.)

2% CNT

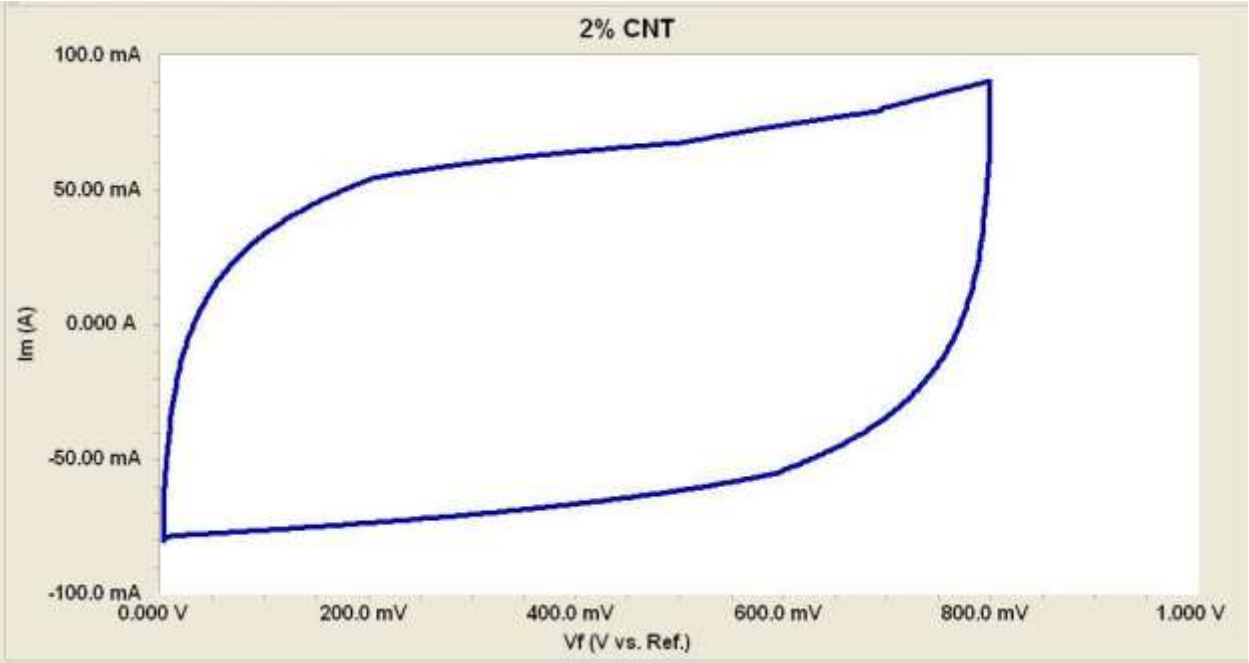
2% CNT
100.0 mA
50.00 mA
0.000 A
-50.00 mA
-100.0 mA
Im (A)
0.000 V
200.0 mV
400.0 mV
600.0 mV
800.0 mV
1.000 V
Vf (V vs. Ref.)

Appendix C – CV Calculations

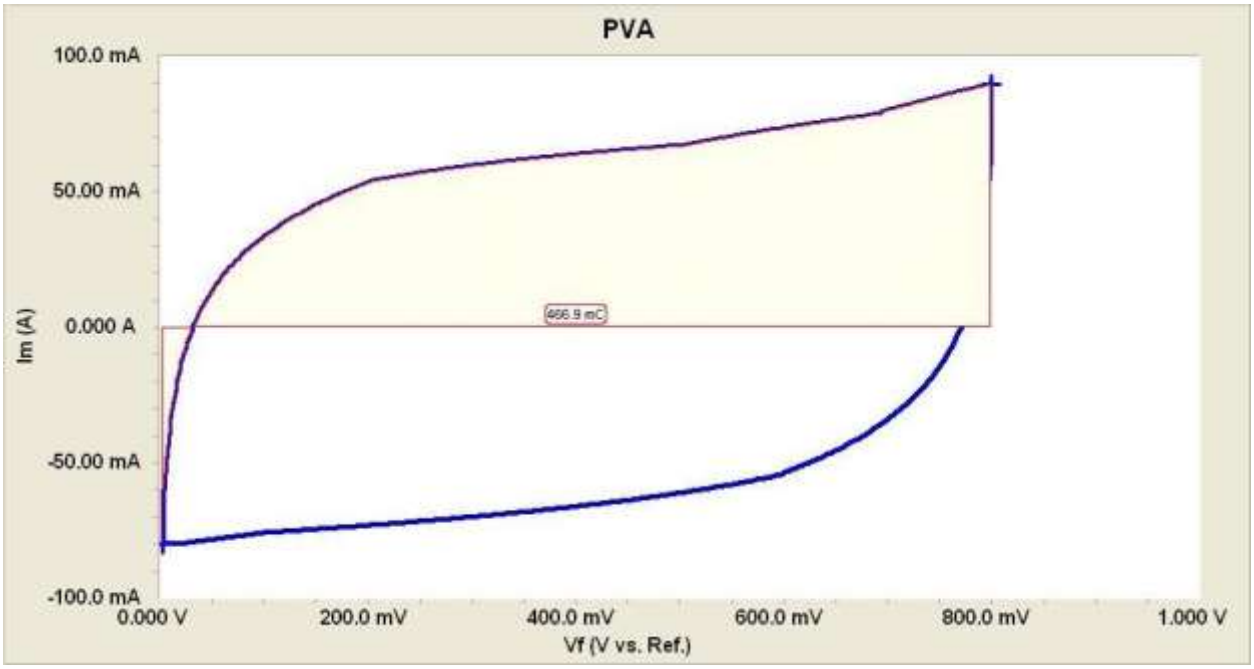

$$C_{(PVA)} = \frac{dQ}{dE} = \left|\frac{Q}{E_2 - E_1}\right| = \frac{0.4669C}{0.8V - 0V} = 0.584F$$

$$C_{s(PVA)} = \frac{C_{(PVA)}}{m} = \frac{0.584F}{0.006g} = 97.27Fg^{-1}$$

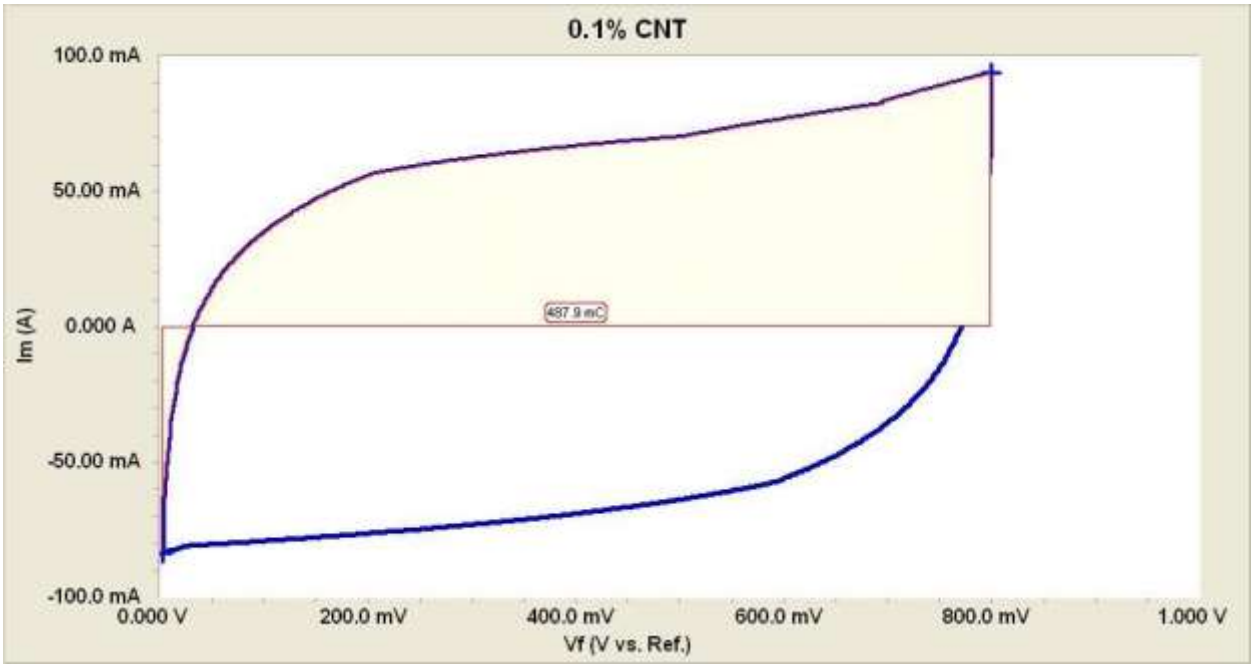

$$C_{(0.1\%)} = \frac{dQ}{dE} = \left|\frac{Q}{E_2 - E_1}\right| = \frac{0.4879C}{0.8V - 0V} = 0.610F$$

$$C_{s(0.1\%)} = \frac{C_{(0.1\%)}}{m} = \frac{0.610F}{0.006g} = 101.65Fg^{-1}$$

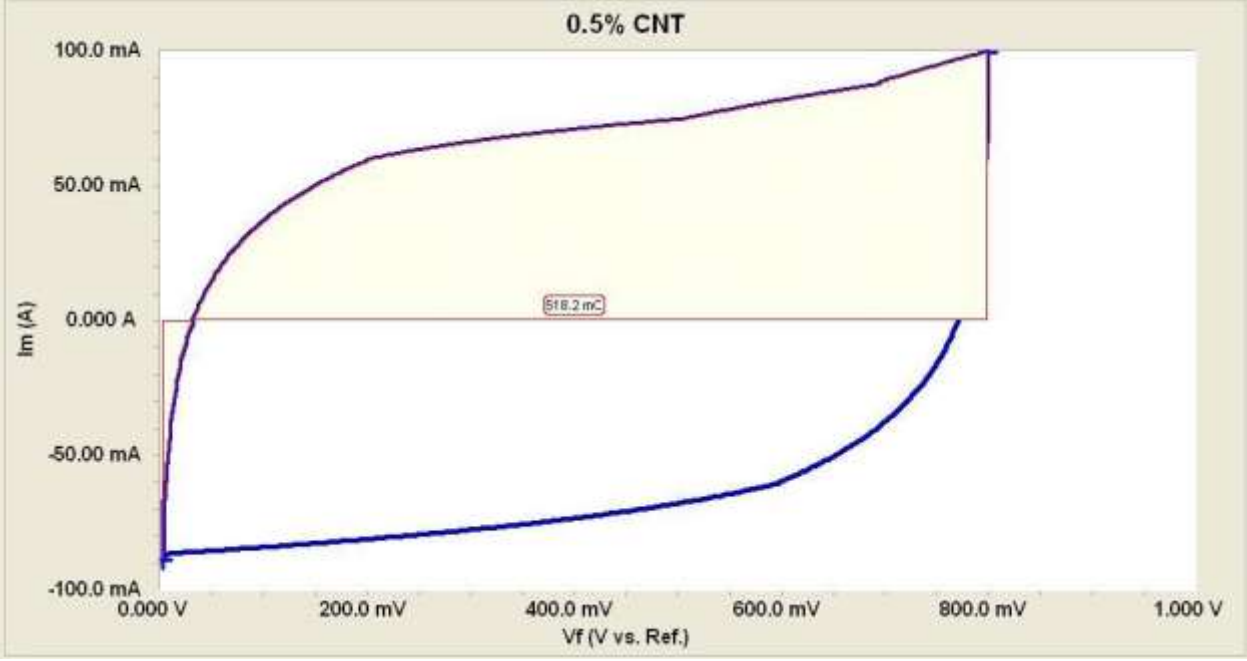

$$C_{(0.5\%)} = \frac{dQ}{dE} = \left|\frac{Q}{E_2 - E_1}\right| = \frac{0.5182C}{0.8V - 0V} = 0.648F$$

$$C_{s(0.5\%)} = \frac{C_{(0.5\%)}}{m} = \frac{0.648F}{0.006g} = 107.96Fg^{-1}$$

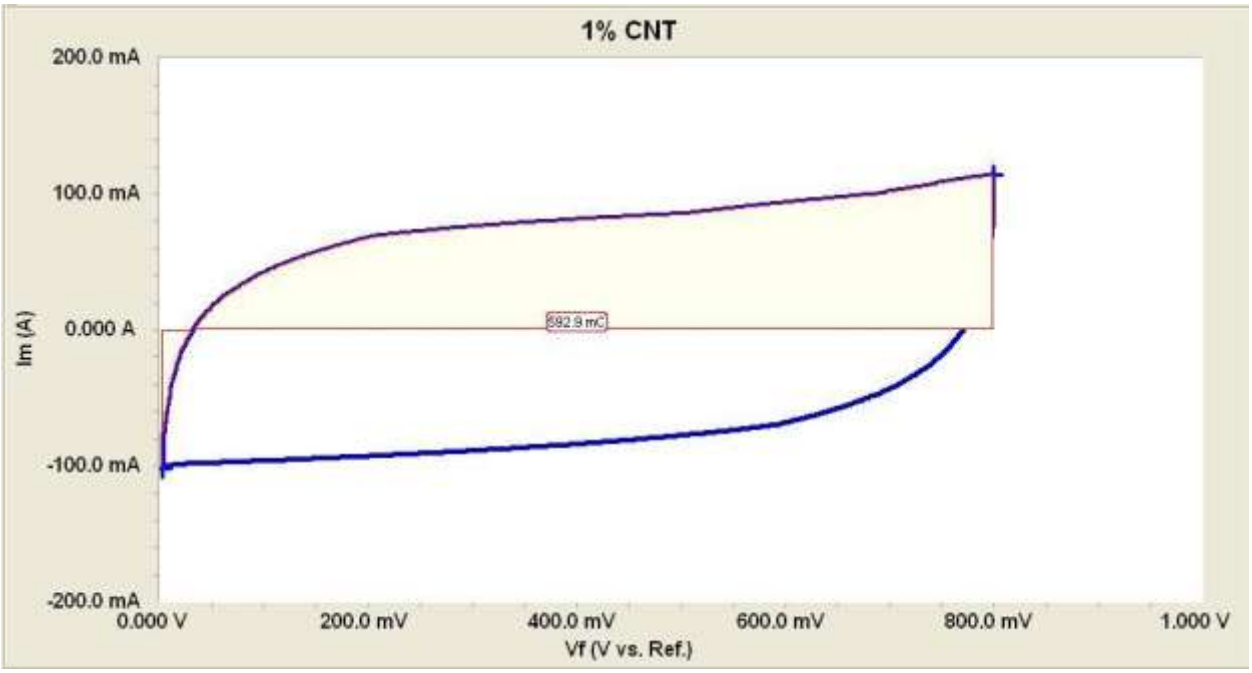

$$C_{(1\%)} = \frac{dQ}{dE} = \left|\frac{Q}{E_2 - E_1}\right| = \frac{0.5929C}{0.8V - 0V} = 0.741F$$

$$C_{s(1\%)} = \frac{C_{(1\%)}}{m} = \frac{0.741F}{0.006g} = 123.52Fg^{-1}$$

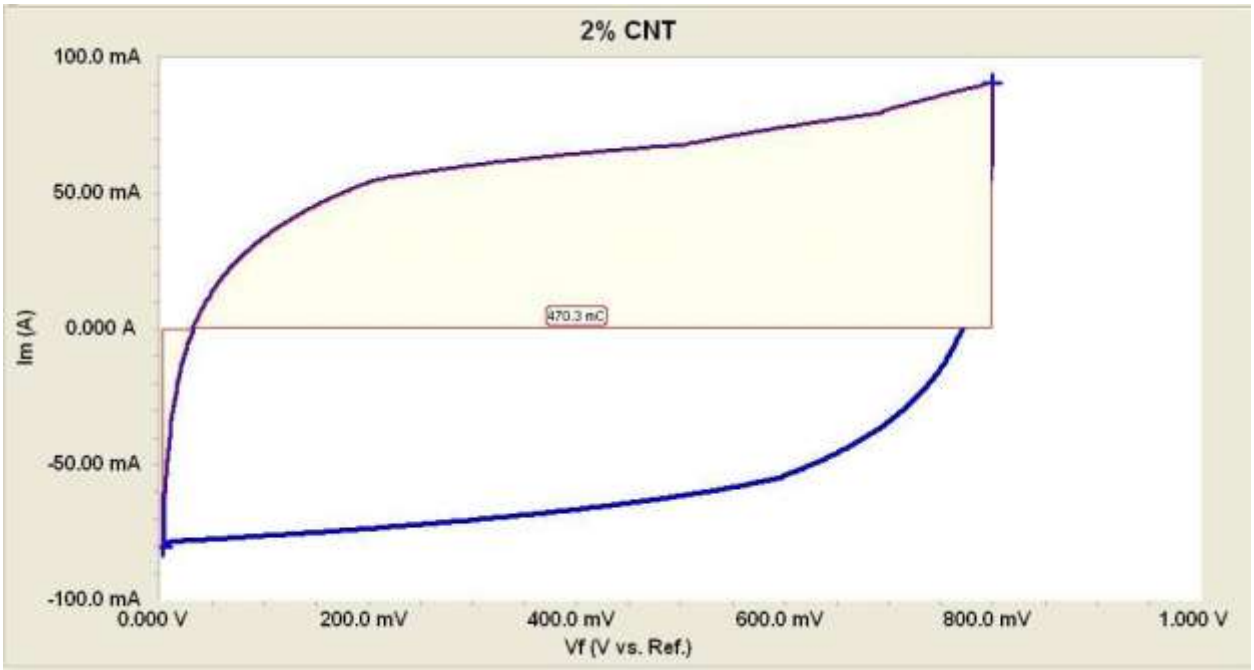

$$C_{(2\%)} = \frac{dQ}{dE} = \left|\frac{Q}{E_2 - E_1}\right| = \frac{0.4703C}{0.8V - 0V} = 0.588F$$

$$C_{s(2\%)} = \frac{C_{(2\%)}}{m} = \frac{0.588F}{0.006g} = 97.98Fg^{-1}$$

Appendix D – Electrolyte Resistivity Calculations

$$R = \rho \frac{l}{A}$$

$$R = \rho \frac{l}{wt}$$

l=2cm, w=2cm

$$R = \rho \frac{l}{wt} = \rho \frac{2cm}{(2cm)t}$$

$$R = \frac{\rho}{t}$$

$$\rho = Rt$$

Electrolyte Type	Resistance (Ω)
PVA	32000±816
0.1% CNT	26000±204
0.5% CNT	42000±216
1% CNT	41000±697
2% CNT	43000±408

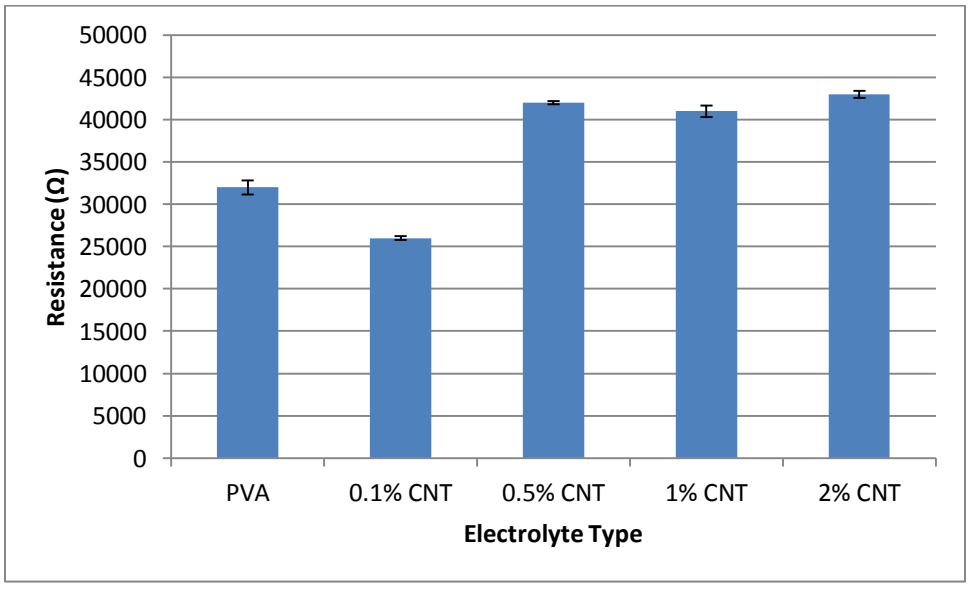

$$\rho_{(PVA)} = Rt = 3.2x10^4\Omega x0.0124cm$$

$$\rho_{(PVA)} = 3.97x10^2\Omega cm$$

$$\rho_{(0.1\%)} = Rt = 2.6x10^4\Omega x0.0149cm$$

$$\rho_{(0.1\%)} = 3.87x10^2\Omega cm$$

$$\rho_{(0.5\%)} = Rt = 4.2x10^4\Omega x0.0070cm$$

$$\rho_{(0.5\%)} = 2.94x10^2\Omega cm$$

$$\rho_{(1\%)} = Rt = 4.1x10^4\Omega x0.0075cm$$

$$\rho_{(1\%)} = 3.06x10^2\Omega cm$$

$$\rho_{(2\%)} = Rt = 4.3x10^4\Omega x0.0077cm$$

$$\rho_{(2\%)} = 3.31x10^2\Omega cm$$